Original research article

I·M3
Institute of Materials, Minerals & Mining

Materials Science and Technology
1–21

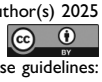
Article reuse guidelines:
sagepub.com/journals-permissions
DOI: 10.1177/02670836251382481
journals.sagepub.com/home/mst
Sage

The role of primary and tertiary creep in defining the form of the Monkman-Grant relation using the 4-θ methodology: An application to 12Cr-Mo-V-Nb steel

Mark Evans[1]

Abstract

It is important to be able to predict the life of materials at high temperatures. The Monkman-Grant relation offers potential for reducing the development cycle for new materials. This paper uses the 4-θ methodology to i. identify and explain the form of this relation in terms of creep mechanisms and ii. to discover whether this form is compatible with development cycle reduction. The Monkman-Grant proportionality constant (M_2) was found to fall into three groupings depending on the amount of damage and the rate at which this occurred. Only once this was considered did the exponent on the secondary creep rate equal −1 – as predicted by 4-θ methodology. One of these groupings might be relevant for longer term life assessment.

Keywords

Monkman-Grant relation, 4-θ methodology, damage, rates of damage accumulation, recovery, hardening

Received: 27 May 2025; accepted: 10 September 2025

Introduction

12Cr-1Mo-V-Nb steel (also referred to as T12 steel or ASTM A387 Grade 12: Class 2 steel) is a type of low-alloy steel that is often classified as a heat-resistant steel. The alloying elements contained within it contribute to its enhanced strength and creep resistance at high temperatures, as well as its good resistance to oxidation and good weldability properties. It is currently used in ultra-super-critical boilers as superheater and reheater tubes that typically operate at temperatures at or above 873 K and stresses exceeding 25 MPa. It is also a material considered for use in advanced nuclear reactors – including fourth generation nuclear reactors. These reactors typically operate in the range 1025 K to 1273 K and a range of 5 to 10 MPa. While it is not commonly used for critical turbine components like blades or rotors, this steel can be used for the parts of turbines that are exposed to less extreme temperatures and stresses where good resistance to creep and oxidation is required.

For the safe and economic operation of such components and systems, a creep rupture life in the time range of 10^5 h is required. Evaluation of such long-term creep rupture is typically done using accelerated creep tests (either accelerated stresses and or temperatures), with creep models then being used to extrapolate to the lower stresses observed in the above-mentioned systems. However, there is little agreement on what creep models extrapolate best with respect to stress and temperature, and whilst some more recently developed models have been shown to perform well at such extrapolation over a wide range of materials, they currently lack the theoretical backing that provides the additional confidence required for widespread adoption (for example, Yang et al.[1] and Wilshire et al.[2–6]). An analysis of minimum creep rates vs. times to failure – the so called Monkman–Grant relation[7] – using accelerated test data is another suggested way to evaluate long-term creep rupture by extrapolating this accelerated relation via smaller minimum creep rates – because once the minimum rate of creep in an on-going creep test at non accelerated stresses is obtained at an early stage of creep, its rupture life is readily evaluated from this accelerated relation without a need to extrapolate with respect to stress and/or temperature.

A relationship between time to failure t_F and the minimum creep rate $\dot{\varepsilon}_M$ was first put forward by Monkman and Grant[7] and is now commonly referred to as the Monkman – Grant relation (or MG for short). They studied several materials (including, but not exclusively, Aluminium, Titanium 75, Ferritic Steels, Austenitic Steels and Inco 700) and identified the following relation

$$t_F = \frac{M}{(\dot{\varepsilon}_M)^{\rho}} \qquad (1a)$$

where these authors found that the parameters ρ and M were constant over all the test conditions contained within the data

[1]Institute of Structural Materials, Swansea University Bay Campus, Swansea, Wales, UK

Corresponding author:
Mark Evans, Institute of Structural Materials, Swansea University Bay Campus, Swansea, Wales SA1 8EN, UK.
Email: m.evans@swansea.ac.uk.

sets that they analysed, but that they differed in value from material to material. (M is frequently termed the Monkman-Grant proportionality constant and ρ the Monkman-Grant exponent). For the materials investigated by these authors, ρ was close to 1 but varied between a low of 0.77 and a high of 0.93 (for Austenitic Steels). Likewise, M varied from a low of 0.48 to a high of 1.3 (for Aluminium). Cocks and Ashby[8] have provided a theoretical explanation of Equation (1a) based on creep-controlled cavity growth.

At a specific test condition, and when $\rho = 1$, the Monkman-Grant equation is a simple tautology or identity (represented by the symbol ≡). Figure 1 shows a hypothetical creep curve containing primary, secondary and tertiary creep obtained at a fixed stress and temperature. The observed minimum creep rate $\dot{\varepsilon}_M$ is equal to the gradient of the creep curve at the point of inflection, and the dashed (upward sloping) line has such a slope – but has been extrapolated to zero time and to the time at failure. By the definition of a gradient, the slope of this line equals the vertical distance M divided by the time to failure t_F

$$\dot{\varepsilon}_M \equiv \frac{M}{t_F} \tag{1b}$$

and so, upon rearranging

$$t_F \equiv \frac{M}{\dot{\varepsilon}_m} \equiv M(\dot{\varepsilon}_M)^{-1} \tag{1c}$$

From this perspective, the Monkman-Grant relation requires the additional assumption that M is the same at all stresses and temperatures (subject to stochastic or random experimental variation). This assumption then turns this simple identity into a useful model or casual relation, because it then follows that a fall in $\dot{\varepsilon}_M$ must led to an increase in the time to failure (rather than to a change in M).

Since this relation was first identified, some doubt has been cast as to the constancy of M and ρ with respect to test conditions. For example, when studying 9Cr-1Mo steel, Abe[9] and Choudary[10] have shown M and ρ are different in value at long failure times (i.e., at lower stresses) compared to short and intermediate failure times. More specifically, these authors found that over most test conditions $\rho = 1$, but at the lower stresses leading to the longest failure times, ρ fell below 1. In order explain the change in values for M and ρ at lower stresses, several modifications of Equation (1a) have been proposed. Dobes and Milicka[11] proposed the following modified form

$$\frac{t_F}{\varepsilon_F} = \frac{M_1}{(\dot{\varepsilon}_M)^{\rho_1}} \text{ with } \rho_1 = 1 \tag{1d}$$

where ϵ_F is the strain at failure. Subsequent authors have found some success with this modification. For example, Sklenicka et al.[12] studied a Grade 92 steel and found a stable value for ρ_1 of 0.96 in Equation (1d) – in contrast to $\rho = 0.88$ in Equation (1a). The MG relation in Equation (1d) is related to the creep damage tolerance parameter λ. This parameter measures the ability of a material to withstand local concentrations of strain accumulation without cracking

$$\lambda = \frac{(\varepsilon_F - \varepsilon_p)}{t_F \dot{\varepsilon}_M} \cong \frac{\varepsilon_F}{t_F \dot{\varepsilon}_M} \cong \frac{1}{M_1} \tag{1e}$$

where ϵ_p is the strain reached at the end of primary creep. The approximation in Equation (1e) corresponds to test conditions where the magnitude and duration of primary creep is small in relation to failure time – $\varepsilon_p \cong 0$. This approximation results in the MG proportionality constant in Equation (1d) being equal to the reciprocal of the damage tolerance parameter, $\lambda^{-1} \cong M_1$. λ values in the range 5–10 are though to ensure that the strain concentrations typically encountered during in service operation will not lead to premature cracking and failure.

Abe[9] attributed the deviation from the simple MG relation with $\rho = 1$ in long-term creep, to increases in $d\ln(\dot{\epsilon})/d\epsilon$, and proposed the following MG relation

$$\frac{d\ln(\dot{\varepsilon})}{d\varepsilon} t_F = \left(\frac{t_F}{(t_F - t_M)}\right)(\dot{\varepsilon}_M)^{-1} \tag{1f}$$

where t_M is the time taken to reach the minimum creep rate, ϵ is the creep strain and $\dot{\varepsilon}$ the creep strain rate. However, when applied to a 9Cr steel, Abe obtained a value for ρ that was still less than 1.

Maruyama et al.[13] have also studied the phenomenon of $\rho < 1$ using data on 9Cr-1Mo (Grade 92) steel. They found that the value for ρ differed over four different regions of stress and temperature, where each of these regions corresponded to different creep mechanisms. Whilst the value for ρ over all tests was 0.85, they found it to be especially low (0.62) in a region corresponding to values of stress and temperature that induced long times to failure (in excess of 10^4 h). With long-term data points deviating from a MG relation determined from short-term data points, it becomes impossible to then use this relationship to evaluate long term life from short term data.

These authors then went onto to study the role played by creep curve shape in determining the values for M and ρ using the following equation

$$\varepsilon = A\ln(1 + \alpha t) - B\ln(1 - \beta t) \tag{2a}$$

where t is time and where A and B are parameters related to strain (i.e., have units %/100), whilst α and β are rate parameters (and have units equal to the inverse of t). A (approximately) measures the decelerating rate of creep during primary creep ($A = -1/(d\ln\dot{\epsilon}/d\epsilon)$), and B measures creep rate acceleration ($B = 1/(d\ln\dot{\epsilon}/d\epsilon)$) in tertiary creep. Hence A and B can be taken as summary measures of creep curve shape. They found that the values of A and B decreased with increasing creep rupture life, and it was this changing shape with t_F that explained the ρ values of less than unity, i.e., ρ is lowest when A and B are lowest. From this analysis they found that constraining M to a value of

$$M = \left(\sqrt{A} + \sqrt{B}\right)^2 \tag{2b}$$

in Equation (1a) resulted in the Monkman-Grant exponent of $\rho = 1$ when applied to all the data on Grade 92 steel (both long and short-term tests results).

However, Equation (2a) is purely empirical in nature and its parameters have not been explained in terms of creep mechanisms. The aim of this paper is to identify a modified Monkman-Grant relation whose parameters can be explained in terms of creep processes such as hardening, softening and damage mechanisms. To do this, a similar material to that

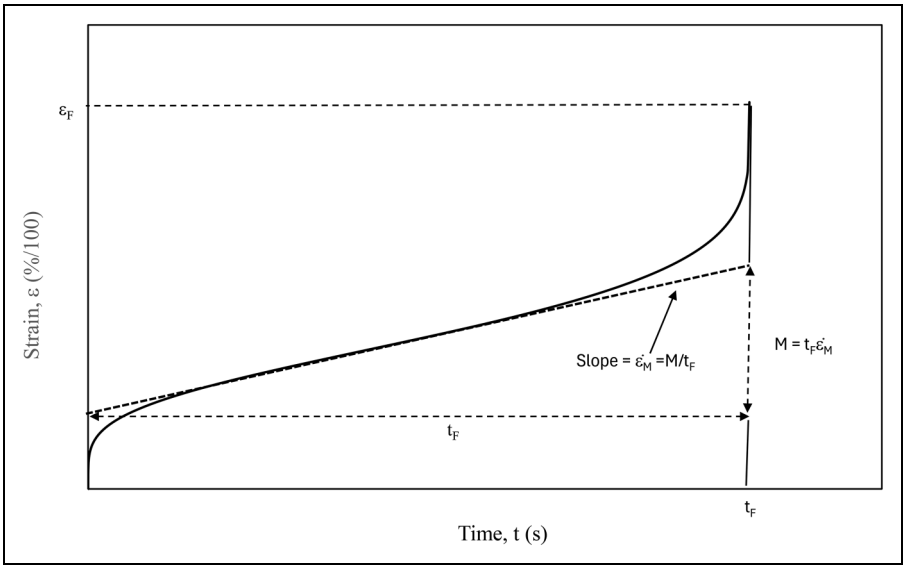

Figure 1. Schematic representation of a uniaxial creep curve obtained at a constant stress and temperature.

studied by Maruyama et al.[13] was selected – namely a Grade 12 steel – but the creep equation used was that from the 4-θ methodology developed by Evans and Wilshire[14]

$$\varepsilon = \theta_1(1 - e^{-\theta_2 t}) + \theta_3(e^{\theta_4 t} - 1) \qquad (2c)$$

where the θ_l are the four theta parameters that relate strain to time. θ_2 and θ_4 are rate parameters and θ_1 and θ_3 scale parameters – so, and for example, the strain obtained by the end of primary creep is given by θ_1. The reason for selecting this methodology is that the form of this equation has already been derived from an analysis of mechanisms governing creep.

The use of the 4-θ methodology enables deviations from the Monkman-Grant relation of Equations (1b, 1c) to be explained not just in terms of creep curve shape, but also mechanisms governing creep. More specifically, this paper will derive a MG relation from the 4-θ methodology to gain insights into the roles played by creep hardening, softening and damage mechanisms in determining the form of the MG relation – and indeed whether these mechanisms change with test conditions. This will then enable insights to be made as to whether and how the MG relation in short term data can be used to evaluate long term rupture. To achieve these aims, the paper is structured as follows. The next section describes the creep tests carried out on Grade 12 steel, and this is followed by a method section outlining how a MG relation can be derived from the 4-θ methodology. This modified relation is then applied to data on 12Cr steel in the results section. Finally, the conclusion section outlines areas for future work.

The data

This section describes the data (which has not been previously published) used in this paper in more detail. Thirty-six cylindrical test pieces were machined from an as received batch of 12Cr-Mo-V-Nb steel. The chemical composition of this batch of material is shown in Table 1. The material was heat treated at 1423 K followed by air cooling and then two rounds of 3 h at 923 K (followed by air cooling each time). The tensile strength (σ_{TS}) for this batch of material is 990 MPa at room temperature and 551 MPa at 873 K, with corresponding 0.2% proof stresses of 831 MPa and 440 MPa. The specimens were tested in tension over a range of stresses and temperatures using high precision in Andrade-Chalmers constant-stress machines at the Interdisciplinary Research Centre (IRC) laboratories at Swansea University. Loads and stresses were applied and maintained to an accuracy of 0.5%. In all cases, temperatures were controlled along the gauge lengths and with respect to time to better than ±1 K. The extensometer could measure tensile strain to better than 10^{-5}. Loading machines, extensometers and thermocouples were all calibrated with respect to NPL traceable standards.

The test matrix used for this paper is shown in Table 2, where it can be noted that at three different test conditions a replicate test was carried out. Up to 403 creep strain/time readings were taken during each of these tests and Figure 2 shows the normalised experimental creep curves obtained at 873 K and various stresses. At these test conditions there are well defined primary and tertiary components to creep and a long period where the creep rate is constant – sometimes referred to as the secondary creep.

Methodology

Creep mechanisms behind the 4-θ methodology

Based on Equation (2c), a specimen on test under uniaxial constant stress and temperature will eventually rupture with a failure time t_F and with a strain at rupture of ϵ_F

$$\varepsilon_F = \theta_1(1 - e^{-\theta_2 t_F}) + \theta_3(e^{\theta_4 t_F} - 1) \qquad (3a)$$

Given that $-\theta_2$ is a small negative number and t_F a large number, $e^{-\theta_2 t_F} \approx 0$ and so

$$\varepsilon_F \approx \theta_1 + \theta_3(e^{\theta_4 t_F} - 1) \qquad (3b)$$

Table 1. Chemical composition (weight %).

Cr	Co	C	Mn	Si	Ni	Mo	Ti	Al	B	V	S	P	Cu
11.2	0.01	0.16	0.74	0.28	0.52	0.51	0.1	0.05	0.008	0.28	0.015	0.022	0.15

Also 0.029 As, 0.065N, 0.29Nb, 0.019Sn and 0.1 W. Balance Fe.

which can be re-arranged for the time to failure

$$t_F \cong \frac{1}{\theta_4}\ln\left[\frac{\varepsilon_F - \theta_1 + \theta_3}{\theta_3}\right] = \frac{1}{\theta_4}\ln\left[1 + \frac{\varepsilon_F - \theta_1}{\theta_3}\right] \cong \frac{1}{\theta_4}\ln\left[1 + \frac{\varepsilon_F - \varepsilon_p}{\theta_3}\right] \quad (3c)$$

where $\epsilon_p \cong \theta_1$ and ϵ_p is the strain accumulated at the end of primary creep. Although not obvious, Equation (3c) is a variant of the Monkman-Grant relation. To see this requires an understanding of the creep mechanisms behind Equation (2c) and this was first outlined by Evans.[15] Following this approach, internal state variables can be used to explain the form of Equation (2c) using as a starting point the following creep constitutive law for the strain rate $\dot{\varepsilon}$

$$\dot{\varepsilon} = \Phi(\sigma, T, \xi_1, \xi_2, \ldots, \xi_\alpha, \ldots, \xi_p) \quad (4a)$$

where σ is stress, T absolute temperature, ξ_α are the internal state variables which are time dependent and $\Phi()$ is (an unknown) functional form. Each of these internal variables will have an equation associated with them to describe their evolution during creep. All the ξ_α describe continuum quantities that could be classified as either hardening or softening, static or dynamic, transitory or permanent. One possible functional form for Equation (4a) is

$$\dot{\varepsilon} = \dot{\varepsilon}_o f(\xi_\alpha) \quad (4b)$$

where $\dot{\varepsilon}_o$ is the initial rate of strain occurring for virgin material when placed on test – and this will depend on both stress and temperature. Here, $f(\xi_\alpha)$ takes on the value one for such material but thereafter is modified by the creep processes occurring within the grains and/or grain boundaries. Next assume that $f(\xi_\alpha)$ is a linear function of these internal variables

$$\dot{\varepsilon} = \dot{\varepsilon}_o\{1 + (h_1 + .. + h_\alpha + .. + h_{mh}) + (r_1 + .. + r_\alpha + .. + r_{mr}) + (w_1 + .. + w_\alpha + .. + w_{mw})\} \quad (4c)$$

where h_α, r_α, and w_α are dislocation hardening, dislocation softening and damage internal variables respectively. Softening (or recovery) variables are those associated with climb and glide and are static but positive variables. On the other hand, hardening variables are dynamic in nature and will be negative in quantity. The damage variables include changes in precipitate morphology, alteration in second-phase interfaces, changes in mobile dislocation density and grain boundary cavitation and cracking – to name a few. They are usually dynamic in nature and positive in quantity. More than one process can occur at a time and each mechanism will be a function of stress and temperature. As the internal variables in Equation (4c) occur linearly, it is possible to define overall hardening, recovery and damage as H, R and W

$$H = \sum_{\alpha=1}^{mh} h_\alpha;\ R = \sum_{\alpha=1}^{mr} r_\alpha \text{ and } W = \sum_{\alpha=1}^{mw} w_\alpha \quad (4d)$$

Evans then postulated the following evolutionary equations for all the internal variables

$$\dot{h}_\alpha = -\hat{h}_\alpha\dot{\varepsilon};\ \dot{w}_\alpha = \hat{w}_\alpha\dot{\varepsilon} \text{ and } \dot{r}_\alpha = \hat{r}_\alpha \quad (4d)$$

where $\hat{h}_\alpha$, $\hat{w}_\alpha$ and $\hat{r}_\alpha$ are positive proportionality constants which are functions of stress and temperature. The dot above each variable refers to the rate of change in this variable with respect to time. Further, as Equation (4d) is linear in the constants $\hat{h}_\alpha$, $\hat{w}_\alpha$ and $\hat{r}_\alpha$, it is also possible to write out evolutionary equations for overall hardening, softening and damage as

$$\dot{H} = -\hat{H}\dot{\varepsilon};\ \dot{R} = \hat{R} \text{ and } \dot{W} = \hat{W}\dot{\varepsilon} \quad (4e)$$

where

$$\hat{H} = \sum_{\alpha=1}^{mh} \hat{h}_\alpha;\ \hat{R} = \sum_{\alpha=1}^{mr} \hat{r}_\alpha \text{ and } \hat{W} = \sum_{\alpha=1}^{mw} \hat{w}_\alpha \quad (4f)$$

Equation (4c) can then be written as

$$\dot{\varepsilon} = \dot{\varepsilon}_o(1 + H + R + W) \quad (4g)$$

Hardening refers to any phenomenon that leads to a slowing down of the creep rate, whilst softening leads to accelerating creep rates. Equation (4g) evaluates creep rates at any point in time relative to the creep rate measured at the start of the test $\dot{\varepsilon}_o$. So, for hardening to reveal itself as declining values for $\dot{\varepsilon}$ over time, H in Equation (4g) must be a negative number. Likewise, for softening to reveal itself as increasing values for $\dot{\varepsilon}$ over time, R in Equation (4g) must be a positive number. At constant stress and temperature, the positive quantities $\hat{H}$, $\hat{R}$, and $\hat{W}$ are also constant. However, it is difficult to a obtain a closed form integral of these equations under all situations, but the shape of the normalised creep curves for 12Cr-Mo-V-Nb steel, seen in Figure 2, suggests that some approximations can be made – which will not significantly affect the modelling results. Figure 2 reveals that i. the duration (in terms of time) of primary creep is very short, ii. most of the creep process consists of secondary creep and iii. there is slow initial acceleration in creep rates

Table 2. Test conditions for each of the 36 cut specimens.

Temperature (K)	Stress (MPa)						
813	440	460	480	500	510		
833	340	390	**410**	460	480		
853	310	325	340	350	360	**390**	460
873	270	308	325	**340**	370		
893	230	250	270	290	310	325	340
923	200	200	250	280			

One specimen was placed on test at each shown condition, except the conditions highlighted in bold – where two specimens were placed on test.

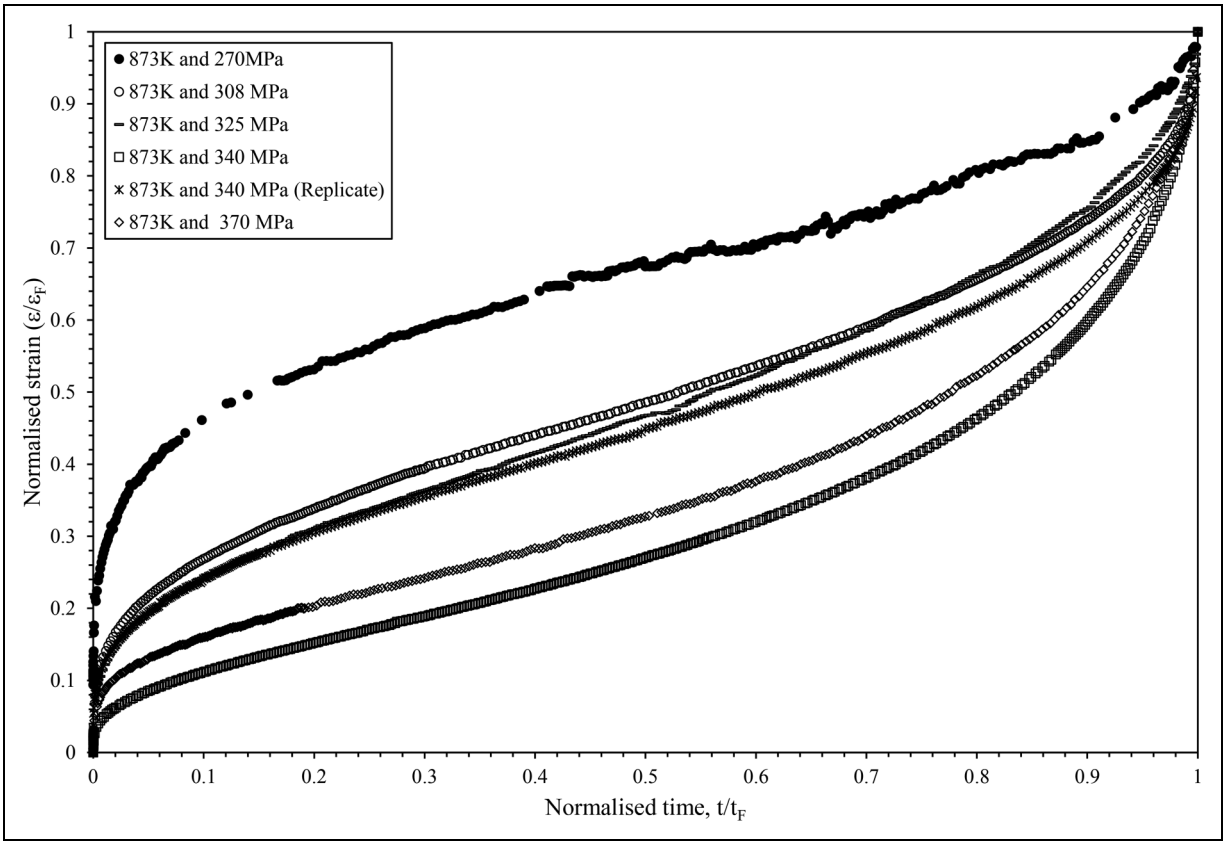

Figure 2. Normalised creep curves obtained from uniaxial tests carried out at 873 K and various stresses.

at the start of tertiary creep. These three characteristics suggests that damage processes are insignificant early in life, and during a lot of tertiary creep.

These characteristics have also been observed by Kafexhiu et al.[16] for this material. For example, these authors noted that at 873 K and 150 MPa, primary creep lasts only a few hours, followed by a prolonged secondary stage. Their long-term data (e.g., 10,000+ hours) showed secondary and tertiary creep domination. Consequently, the value of W in Equation (4g) remains close to zero for a large proportion of the overall creep time, so that the primary and secondary creep strain rate can be modelled as

$$\dot{\varepsilon} = \dot{\varepsilon}_o(1 + H + R) \tag{4h}$$

without any significant loss of accuracy. Now, H = R = W = 0 when t = 0, so the differential of Equation (4h) with respect to time is

$$\ddot{\varepsilon} = \dot{\varepsilon}_o(\dot{H} + \dot{R}) = \dot{\varepsilon}_o(\hat{R} - \hat{H}\dot{\varepsilon}) \tag{5a}$$

for small times in relation to creep life, i.e., where the effects of W are negligible. The creep rate is found by performing the following integration

$$\int_{\dot{\varepsilon}_o}^{\dot{\varepsilon}} \frac{1}{(\hat{R} - \hat{H}\dot{\varepsilon})} d\dot{\varepsilon} = \dot{\varepsilon}_o \int_0^t dt$$

to give

$$\ln[(\hat{R} - \hat{H}\dot{\varepsilon})] + C = -\hat{H}\dot{\varepsilon}_o t$$

where C is the constant of integration. When t = 0, $\dot{\varepsilon} = \dot{\varepsilon}_o$ and so C = -ln $(\hat{R} - \hat{H}\dot{\varepsilon}_o)$. Thus

$$\ln\left[\frac{(\hat{R} - \hat{H}\dot{\varepsilon})}{(\hat{R} - \hat{H}\dot{\varepsilon}_o)}\right] = -\hat{H}\dot{\varepsilon}_o t \tag{5b}$$

Next exponentiate both sides and then multiple both sides by $\hat{R} - \hat{H}\dot{\varepsilon}_o$ to give

$$\hat{R} - \hat{H}\dot{\varepsilon} = (\hat{R} - \hat{H}\dot{\varepsilon}_o)e^{-\hat{H}\dot{\varepsilon}_o t} \tag{5c}$$

Then solving for $\hat{H}\dot{\varepsilon}$ and dividing both sides by $\hat{H}$ gives

$$\dot{\varepsilon} = \frac{\hat{R}}{\hat{H}} - \left(\frac{\hat{R} - \hat{H}\dot{\varepsilon}_o}{\hat{H}}\right)e^{-\hat{H}\dot{\varepsilon}_o t} \tag{5d}$$

Then distribute and rearrange to yield

$$\dot{\varepsilon} = \left[\dot{\varepsilon}_o - \frac{\hat{R}}{\hat{H}}\right]e^{-\hat{H}\dot{\varepsilon}_o t} + \frac{\hat{R}}{\hat{H}} \tag{6a}$$

Equation (6a) states that an initial high creep rate of $\dot{\varepsilon}_o$ gives way to a rapidly decreasing creep rate until a steady state rate of creep equal to $\frac{\hat{R}}{\hat{H}}$ is reached. This can be interpreted as the theoretical secondary creep rate – that rate that would be observed if creep continued to progress without meaningful damage accumulation. Call this rate $\dot{\varepsilon}_S$ and so

$$\dot{\varepsilon}_S = \frac{\hat{R}}{\hat{H}} \tag{6b}$$

The value for this secondary creep rate is determined by the rate of work hardening $\hat{H}$ in relation to the rate of softening $\hat{R}$ occurring during primary creep. This is a very general specification of creep to which a variety of different creep

mechanisms can be attached. Without this simplifying assumption, (i.e., integrating Equation (4g)), Equation (6a) becomes

$$\dot{\varepsilon} = \left[\dot{\varepsilon}_o + \frac{\hat{R}}{\hat{W}-\hat{H}}\right]e^{-\hat{H}\dot{\varepsilon}_o t} - \frac{\hat{R}}{\hat{W}-\hat{H}} \qquad (6c)$$

Now the secondary creep rate is determined by the rate of recovery relative to the excess of the hardening rate over the damage rate $\frac{\hat{R}}{\hat{W}-\hat{H}}$. But for Equation (6c) to have the characteristics of the creep curves shown in Figure 2, $(\hat{W}-\hat{H})<0$. Then at the start of a creep test (t = 0), the rate of strain is given by $\dot{\varepsilon}_o$ (as $e^o = 1$) and subsequently $\dot{\varepsilon}$ will reduce in value until a value of $\frac{\hat{R}}{(\hat{W}-\hat{H})}$ is reached. But for this to happen rapidly as presented in Figure 2, $\hat{W}$ must also be very small relative to $\hat{H}$. That is, damage accumulation in minimal during primary creep, or $-\frac{\hat{R}}{(\hat{W}-\hat{H})}$ approximately equals $\frac{\hat{R}}{\hat{H}}$ and so can replace $\frac{\hat{R}}{\hat{W}-\hat{H}}$ in Equation (6c). This simplifying assumption does not affect the results presented later on. All it means is that when referring to the hardening rate, what is really meant is hardening net of any primary damage. This simplifying approach does not mean that damage is confined to tertiary creep. Instead, it means damage generation is restricted to those strains arising from the secondary creep process, which of course is present throughout the whole of primary creep.

The Monkman-Grant relation and damage

A second key assumption behind Equation (2c), that is also key to a more in depth understanding of the Monkman-Grant relation, is that damage W leads to strain rate accumulation by accelerating the secondary creep rate $\dot{\varepsilon}_S$

$$\dot{\varepsilon} = \left[\dot{\varepsilon}_o - \frac{\hat{R}}{\hat{H}}\right]e^{-\hat{H}\dot{\varepsilon}_o t} + \frac{\hat{R}}{\hat{H}}[1+W] \qquad (7a)$$

or, upon extracting all primary creep

$$\dot{\varepsilon}_T = \frac{\hat{R}}{\hat{H}}\,[1+W] \qquad (7b)$$

where $\dot{\varepsilon}_T$ is the tertiary strain rate. This can be rewritten in terms of time t by first noting that

$$\ddot{\varepsilon}_T = \frac{\hat{R}}{\hat{H}}\,[\dot{W}] = \frac{\hat{R}}{\hat{H}}\hat{W}\dot{\varepsilon}_T \qquad (7c)$$

The next step is to perform an integration over the times and strains associated with tertiary creep

$$\int_{\dot{\varepsilon}_s}^{\dot{\varepsilon}_F} \frac{1}{\left(\hat{W}\dot{\varepsilon}_T\right)} d\dot{\varepsilon}_T = \frac{\hat{R}}{\hat{H}}\int_{t_p}^{t} dt$$

where t_p is time taken to reach the end of primary creep. This leads to

$$\frac{1}{\hat{W}}\ln[\dot{\varepsilon}_T] = \frac{\hat{R}}{\hat{H}}(t-t_p) + C \qquad (7d)$$

When $t = t_p$ the initial tertiary creep rate will equal the steady state creep rate, i.e., $\frac{\hat{R}}{\hat{H}} = \dot{\varepsilon}_T$ and so $C = \frac{1}{\hat{W}}\ln\left[\frac{\hat{R}}{\hat{H}}\right]$.

Upon further simplification

$$\dot{\varepsilon}_T = \frac{\hat{R}}{\hat{H}}e^{\frac{\hat{R}}{\hat{H}}\hat{W}(t-t_p)} \qquad (7e)$$

But for this material, Figure 2 reveals that t_p is very small relative to t_F so that $(t-t_p) \cong t$. Under this approximation and substituting this into Equations (7a, b), gives

$$\dot{\varepsilon} = \left[\dot{\varepsilon}_o - \frac{\hat{R}}{\hat{H}}\right]e^{-\hat{H}\dot{\varepsilon}_o t} + \frac{\hat{R}}{\hat{H}}e^{\frac{\hat{W}\hat{R}}{\hat{H}}t} \qquad (8a)$$

which upon integration results in the 4-θ creep curve

$$\varepsilon = \frac{1}{\hat{H}\dot{\varepsilon}_o}\left[\dot{\varepsilon}_o - \frac{\hat{R}}{\hat{H}}\right](1-e^{-\hat{H}\dot{\varepsilon}_o t}) + \frac{1}{\hat{W}}\left(e^{\frac{\hat{W}\hat{R}}{\hat{H}}t} - 1\right) \qquad (8b)$$

An important advantage of this theta methodology is that all the internal variables can be easily and directly calculated from the θ values describing a uniaxial creep curve. So, comparing Equations (8b) to (2c), it follows that

$$\dot{\varepsilon}_o = \theta_1\theta_2 + \theta_3\,\theta_4;\ \hat{W} = \frac{1}{\theta_3};\ \hat{H} = \frac{\theta_2}{\dot{\varepsilon}_o};\ \hat{R} = \frac{\theta_2\theta_3\theta_4}{\dot{\varepsilon}_o} \qquad (8c)$$

This approach makes it particularly useful for finite element modelling of more complex structures and situations where the stress is continually changing during the deformation process – e.g., in modelling the small punch test. Instead of using strain, time or life fraction hardening rules in such models, the estimated theta parameters can be used to recompute H, R and W, when there are changes in stress – which in combination with Equation (4g) allows the new point on the new stress creep rate curve to be quantified.

Equation (8c) is another way of showing that the two assumptions or approximations made in the derivation of Equations (8a, 8b) do not remove the appearance of damage from primary creep. In Equation (8c) θ_3 determines the rate of damage accumulation $\widehat{W}$. But θ_3 also determines, in part, the values for $\hat{R}$ *and* $\dot{\varepsilon}_o$ and thus $\hat{H}$ and so it follows that the rate of damage accumulation also controls primary creep. So, the assumptions only restrict damage generation to those strains arising from the secondary process, which is present throughout the whole of primary. It is these assumptions that directly leads to or implies the existence of the well-established Monkman-Grant relationship that relates fracture behaviour to the product of the secondary creep rate and failure time rather than total strain.

From Equation (8c) $\theta_4 = \hat{W}\frac{\hat{R}}{\hat{H}} = \hat{W}\,\dot{\varepsilon}_S$ and $\theta_3 = 1/\hat{W}$ and so $\dot{\varepsilon}_S = \frac{\hat{R}}{\hat{H}} = \theta_3\,\theta_4$. Using this measure of the minimum creep rate allows Equation (3c) to be written as

$$t_F \approx \frac{1}{\theta_4}\ln\left[1 + \frac{\varepsilon_F - \varepsilon_p}{\theta_3}\right] = \theta_3\ln\left[1 + \frac{\varepsilon_F - \varepsilon_p}{\theta_3}\right](\dot{\varepsilon}_S)^{-1} \qquad (9a)$$

This is a Monkman-Grant type relation with $M = \theta_3\ln\left[1 + \frac{\varepsilon_F - \varepsilon_p}{\theta_3}\right]$. To further interpret the meaning of M, it can be noted that the amount of damage accumulated by the time of failure W_F can be calculate from Equation (7a)

$$\dot{\varepsilon}_F = \left[\dot{\varepsilon}_o - \frac{\hat{R}}{\hat{H}}\right]e^{-\hat{H}\dot{\varepsilon}_o t_F} + \frac{\hat{R}}{\hat{H}}[1+W_F] \cong \frac{\hat{R}}{\hat{H}}[1+W_F] \qquad (9b)$$

where $\dot{\varepsilon}_F$ is the strain rate at failure and W_F is the total amount of damage accumulated by time t_F. But from Equation (8a)

$$\dot{\varepsilon}_F = \left[\dot{\varepsilon}_o - \frac{\hat{R}}{\hat{H}}\right]e^{-\hat{H}\dot{\varepsilon}_o t_F} + \frac{\hat{R}}{\hat{H}}e^{\frac{\hat{W}\hat{R}}{\hat{H}}t_F} \cong \frac{\hat{R}}{\hat{H}}e^{\frac{\hat{W}\hat{R}}{\hat{H}}t_F} \qquad (9c)$$

From Equations (9b, 9c)

$$\frac{\hat{R}}{\hat{H}}[1 + W_F] = \frac{\hat{R}}{\hat{H}}e^{\frac{\hat{W}\hat{R}}{\hat{H}}t_F}$$

or

$$[1 + W_F] = e^{\frac{\hat{W}\hat{R}}{\hat{H}}t_F} \qquad (9d)$$

As an approximation

$$\varepsilon_p = \theta_1(1 - e^{-\theta_2 t_p}) + \theta_3(e^{\theta_4 t_p} - 1) \approx \theta_1$$

and then using Equation (3b) it follows that

$$\varepsilon_F - \varepsilon_p = \theta_1 + \theta_3(e^{\theta_4 t_F} - 1) - \theta_1 = \frac{1}{\hat{W}}\left(e^{\frac{\hat{W}\hat{R}}{\hat{H}}t_F} - 1\right) \qquad (9e)$$

Substituting Equations (9d) into (9e)

$$\varepsilon_F - \varepsilon_p = \frac{1}{\hat{W}}W_F$$

and upon rearrangement for W_F

$$W_F = \hat{W}(\varepsilon_F - \varepsilon_p) \qquad (9f)$$

Evans[15] made it clear that W_F does not have any units and it therefore dimensionless. Thus, what is consider a high value for W_F is material specific. At first sight this raises concerns about physical interpretation, but past studies on other materials such as Waspaloy[17,18] and have shown that W_F depends directly on stress and indirectly on temperature via the material's tensile strength. Such a functional relationship can then be used to calculate the damage level that will induce failure at any test condition, and thus when failure will occur.

This then allows Equation (9a) to be written as

$$t_F \approx \frac{1}{\hat{W}}\ln[1 + W_F](\dot{\varepsilon_S})^{-1} = M_2(\dot{\varepsilon_S})^{-1} \qquad (10)$$

which is a Monkman-Grant relation of Equation (1a) with $M = M_2 = \frac{1}{\hat{W}}\ln[1 + W_F]$, $\rho = 1$ and the minimum creep rate $\dot{\varepsilon}_M$ replaced with the theoretical secondary creep rate $\dot{\varepsilon}_S$. The MG constant M_2 will only be a true constant if both $\hat{W}$ and W_F are independent of test conditions. But $\hat{W}$ is the reciprocal of θ_3 which is known to be weakly dependent on test conditions, whilst W_F depends on ε_F and θ_1 which are also weakly dependent on test conditions.

The role of primary creep in the determination of time to failure is limited to $\dot{\varepsilon}_S$, which in turn is determined by the rate of hardening relative to the rate of recovery. The larger is the rate of recovery relative to the rate of hardening, the higher will be the secondary creep rate and consequently the smaller will be the time taken to fail. Equation (10) also makes it clear that the Monkman-Grant constant M_2 depends on several factors. Tertiary creep determines the time to failure through the amount of damage accumulated during tertiary creep and the rate at which this damage accumulates. The version of the Monkman-Grant relation given by Equation (10) results from the assumed mechanism that the role of damage accumulation in creep is to accelerate the secondary creep rate $\dot{\varepsilon}_S$. From Equation (10) it follows that failure times will be larger for a given secondary creep rate (i.e., M_2 will be larger) the more ductile is the material, i.e., the greater is the amount of tertiary strain $\varepsilon_F - \varepsilon_p$ and damage W (in the form of voids, precipitate morphology, alteration in grain boundary cavitation and cracking etc) that the material can absorb before failing. So, in the 4-θ version of the Monkman-Grant relation, ϵ_F plays a role but in a different way to that proposed by Dobes and Milicka. The effect of a change in the rate of damage accumulation on M_2 is less clear because an increase in $\hat{W}$ will increase W_F but decrease $1/\hat{W}$. It can be shown that the derivative of M_2 with respect to $\hat{W}$ is negative (see Appendix 1), and so an increase in the rate of damage accumulation will decrease the failure time at a given secondary creep rate.

In summary, the 4-θ methodology suggests M_2 will be larger the more the material can tolerate significant creep strain or stress relaxation before damage (e.g., voids, microcracks) leads to failure. It also suggests that M_2 will be larger the slower this damage accumulates over time. So, whether M_2 is independent of test conditions, depends on whether this materials ability to tolerate damage (and that rate of its accumulation over time) is determined by the test condition. Past studies on other materials such as Waspaloy[17,18] and have shown that W_F depends directly on stress and indirectly on temperature via the material's tensile strength. The results section later will look at this in more detail.

Measuring minimum creep rates

The actual or observed creep rate at a given test condition is measured from the experimental creep curve. If such a curve is made up of i = 1 to n strain-time pairings, then the first step is to create a smoothed series for the experimental rates of strain using

$$\dot{\varepsilon}_i = \left\{\frac{9\sum_{i=-4}^{4}\varepsilon_i t_i - \sum_{i=-4}^{4}\varepsilon_i \sum_{i=-4}^{4} t_i}{9\sum_{i=-4}^{4} t_i^2 - \sum_{i=-4}^{4}(t_i)^2}\right\} \qquad (11)$$

where the subscript on t and ϵ denotes to the ith measurement made for time and strain respectively. Thus, the creep rate at time t_i is found by collecting the pairing $t_i\epsilon_i$, the four $t_i\epsilon_i$ pairings immediately below $t_i\epsilon_i$ and the four $t_i\epsilon_i$ pairings immediately above $t_i\epsilon_i$ and putting a least squares linear line fit through these 9 data points. $\dot{\varepsilon}_i$ is then the slope of this best fit line.

Figure 3 shows this smoothed experimental strain rate obtained at 440 MPa and 813 K. The observed minimum creep rate is not taken to be the smallest observed value, but the mean of the strain rates along the flat part of the strain rate curve. This observed minimum strain rate is what is usually shown in papers when studying the Monkman-Grant relation and is therefore represented by the symbol $\dot{\varepsilon}_M$ (although authors use variations of the smoothing technique given by Equation (11)). For this test condition, the observed minimum creep rate is estimated at 2.52E-09 s^{-1}. Such an estimate has a strong subjective component, because it is

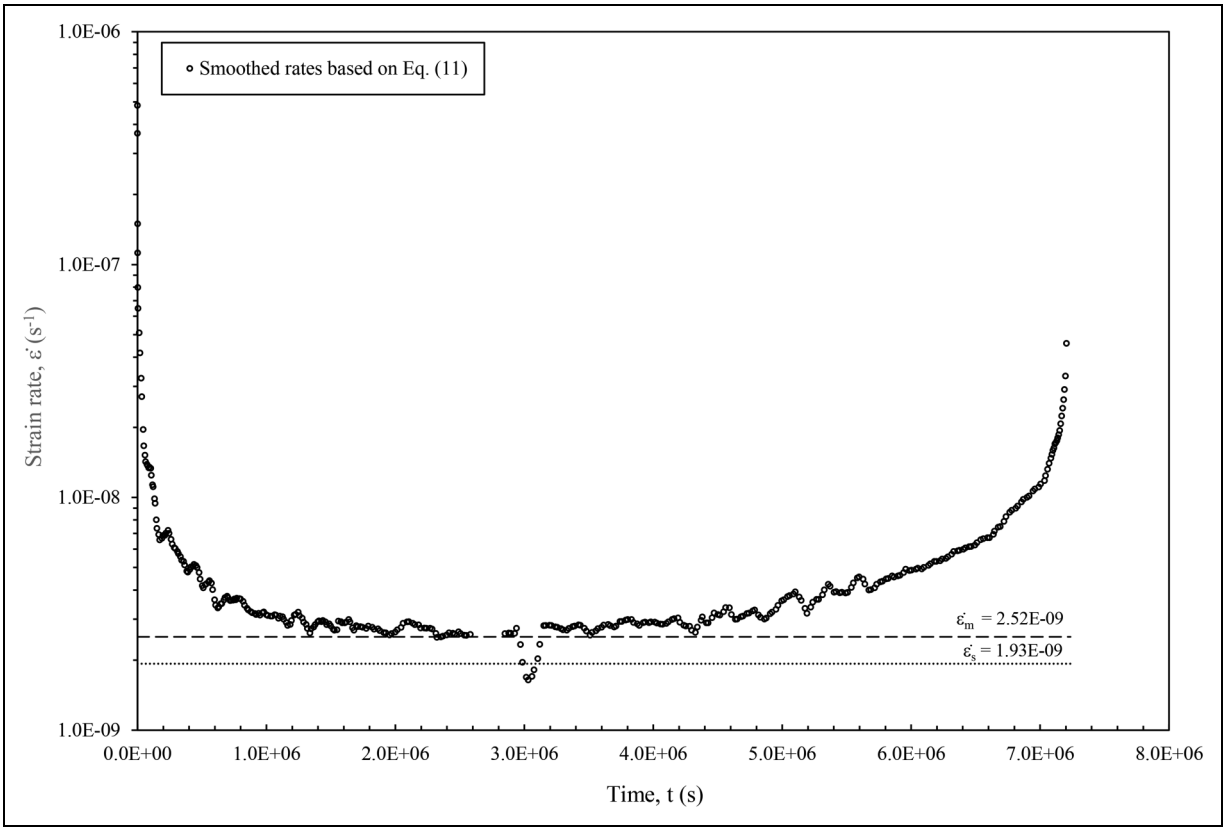

Figure 3. Smoothed experimental strain rates at 440 MPa and 813 K obtained using Equation (11), together with an estimate for the minimum creep rate and theoretical secondary rate.

down to the researcher to identify exactly when the flat part of the curve starts and ends.

In contrast to this, the theoretical secondary rate $\dot{\varepsilon}_S$ cannot be directly measured from the actual experimental creep curve when there is damage accumulating. Instead, Equation (2c) must be fitted to this experimental curve, to obtain estimates for θ_1 to θ_4 – see Evans[19] for details on such appropriate estimation or curve fitting techniques. If such estimates for θ_1 to θ_4 are represented by $\tilde{\theta}_1$ to $\tilde{\theta}_4$, then $\dot{\varepsilon}_S$ can be calculated as

$$\dot{\varepsilon}_S = \frac{\hat{R}}{\hat{H}} = \tilde{\theta}_3\tilde{\theta}_4 \qquad (12a)$$

The rate of damage accumulation can be measured as

$$\hat{W} = \frac{1}{\tilde{\theta}_3} \qquad (12b)$$

and so

$$\frac{\hat{R}}{\hat{H}}\hat{W} = \tilde{\theta}_4 \qquad (12c)$$

All the other internal rates can also be measured from the parameters of the fitted creep curve

$$\dot{\varepsilon}_o = \tilde{\theta}_1\tilde{\theta}_2 + \tilde{\theta}_3\tilde{\theta}_4;\ \hat{H} = \frac{\tilde{\theta}_2}{\dot{\varepsilon}_o};\ \hat{R} = \frac{\tilde{\theta}_2\tilde{\theta}_3\tilde{\theta}_4}{\dot{\varepsilon}_o} \qquad (12d)$$

At 440 MPa and 813 K the estimates for θ_3 and θ_4 are $\tilde{\theta}_3 = 0.01436$ and $\tilde{\theta}_4 = 1.345\text{E}-07$ and so $\tilde{\theta}_3\tilde{\theta}_4 = 1.93\text{E}-09$. There is no reason for $\dot{\varepsilon}_S$ to exactly equal $\dot{\varepsilon}_M$ as the former measure depends only on the rates of hardening and recover, whilst the latter measure obtained from the actual creep curve will contain some contributions from damage. If creep carried on without any damage the creep strain rates seen in Figure 3 would tend to the limit $1.93\text{E}-09-$ which is slightly lower than that seen in the experimental curve where damage is contributing to the actual rates. They should however be similar in value at most test conditions (unless the damage rate is large early on).

Results

Estimated values for each theta parameter and rates of hardening, softening and damage

Table 3 summarises the estimated values for each theta parameter at each test condition. These values are then inserted into Equations (12b, 12c, 12d) to obtain values for the rates of hardening, softening and damage. Such values are visualised in Figures 4–6.

Figure 4(a) shows the estimates made for the proportionality constant determining the hardening rate at each test condition, together with the weighted isothermal best fit lines. The weights used are the inverses of the values given in Figure 4(b) where the ratio of each hardening constant to its standard deviation are plotted. Irrespective of temperature, decreasing stress tends to lead to an increase in the hardening constant, as so other things being equal, to a lower minimum creep rate and a smaller reduction in the creep rate as time progresses during tertiary creep. Typically, the standard deviation associated with each hardening constant is around 1% of the estimated value, but at 873 K, two of the hardening

Table 3. Estimated theta values by test condition.

Stress, MPa	Temperature, K	$\tilde{\theta}_1$	$\tilde{\theta}_2$	$\tilde{\theta}_3$	$\tilde{\theta}_4$
510	813	0.01054	0.00016615	0.00801	1.9791E-05
500	813	0.01028	0.00020146	0.02448	8.2971E-06
480	813	0.01069	2.5068E-05	0.01273	1.343E-06
460	813	0.00889	1.988E-05	0.01189	7.4097E-07
440	813	0.00666	8.491E-06	0.01436	1.3447E-07
480	833	0.00995	0.00041659	0.01833	2.2724E-05
460	833	0.00854	5.3139E-05	0.00614	5.1935E-06
410	833	0.00792	1.7525E-05	0.0067	6.884E-07
410	833	0.00597	1.297E-05	0.00669	6.5006E-07
390	833	0.0075	2.0774E-05	0.00806	2.3159E-07
340	833	0.00554	3.563E-06	0.86832	3.6217E-10
460	853	0.01287	0.00025382	0.00769	6.1161E-05
390	853	0.00684	2.7416E-05	0.00327	2.1693E-06
390	853	0.01243	5.3234E-06	0.00072	2.617E-06
360	853	0.00611	2.0563E-05	0.01029	3.2423E-07
350	853	0.00565	5.8522E-05	0.00192	6.6526E-06
340	853	0.00542	4.6017E-05	0.00376	1.6486E-06
325	853	0.0051	0.00010074	0.01633	3.3565E-07
310	853	0.00369	9.8097E-06	0.2097	3.2242E-09
370	873	0.00568	0.00018246	0.0044	6.9103E-06
340	873	0.0064	9.8269E-05	0.00152	2.3474E-05
340	873	0.00414	0.00012419	0.02151	4.4123E-07
325	873	0.00574	4.1323E-05	0.01187	9.0376E-07
308	873	0.00466	4.2564E-05	0.00968	8.2186E-07
270	873	0.00673	1.4702E-05	0.17644	9.0799E-09
340	893	0.00386	0.00062522	0.00646	1.8244E-05
325	893	0.00532	0.00082874	0.00249	2.0432E-05
310	893	0.00639	0.00024859	0.00302	1.3371E-05
290	893	0.00276	0.00026115	0.15098	2.236E-07
270	893	0.00392	9.4681E-05	0.47025	1.7503E-08
250	893	0.00309	1.7497E-05	0.31433	4.0979E-09
230	893	0.00253	5.7519E-05	0.19305	1.5772E-08
280	923	0.00487	0.00018039	0.00287	1.2E-05
250	923	0.00311	5.5048E-05	0.00155	4.8356E-06
220	923	0.00454	3.9107E-05	0.00363	1.0361E-06
200	923	0.00378	8.7576E-05	0.00393	5.8287E-07

constant estimates are very unreliable and at 853 K one hardening constant estimate is unreliable as revealed by very high ratios in Figure 4(b). These three data points therefore play a small role in the determination of the shape of the weighted best fit lines.

Figure 4(a) reveals that the hardening constant declines with increases in both stress and temperature. Han et. al.[20] found that in 12Cr-1Mo-V-Nb steels, increased stress and temperature accelerate the coarsening of MX precipitates, leading to a decrease in the material's resistance to creep deformation. This coarsening reduces the effectiveness of precipitate strengthening, resulting in lower creep hardening rates. Higher stresses and temperatures can lead to the annihilation of dislocations, reducing the dislocation density. Since dislocations contribute to work hardening, their reduction leads to a decrease in the material's ability to harden during creep deformation.

Figure 5(a) shows the estimates made for the proportionality constant determining the softening rate at each test condition, together with the weighted iso-thermal best fit lines. Figure 5(b) plots the ratio of each softening rate to its standard deviation. Unlike for the hardening, the effect of an increase in stress at a given temperature is to increase the softening constant. Broadly speaking, temperature tends to shift these iso-thermal best fit lines in a parallel fashion. The exception to this is at 893 K – but the weights are such that only three data points play a significant role in positioning this iso-thermal line (and so its slope is subject to more uncertainty). Typically, the standard deviation associated with each softening constant is between 1 and 10% of the estimated value, but there are around five softening constants whose standard deviation is equal to or more than the actual estimated value.

Figure 5(a) shows that the proportionality constant increase with stress at this temperature. Several studies on this material have also observed this phenomenon. The study by Pešička[21] found for this alloy that during creep at 923 K, the mean sub grain size increased under both high and low initial stress levels. Notably, carbide particle coarsening was more pronounced at the lower stress level, suggesting that higher stresses can accelerate softening processes. Further, a study by Dudova[22] indicated that the evolution of lath width during creep depends on the stability of precipitates located on the lath boundaries. The study found that a sharp increase in lath width or sub grain size above 1μm usually corresponds to the transformation of the lath structure into a sub grain structure, which is more likely to occur under higher stress conditions. These studies underscore the

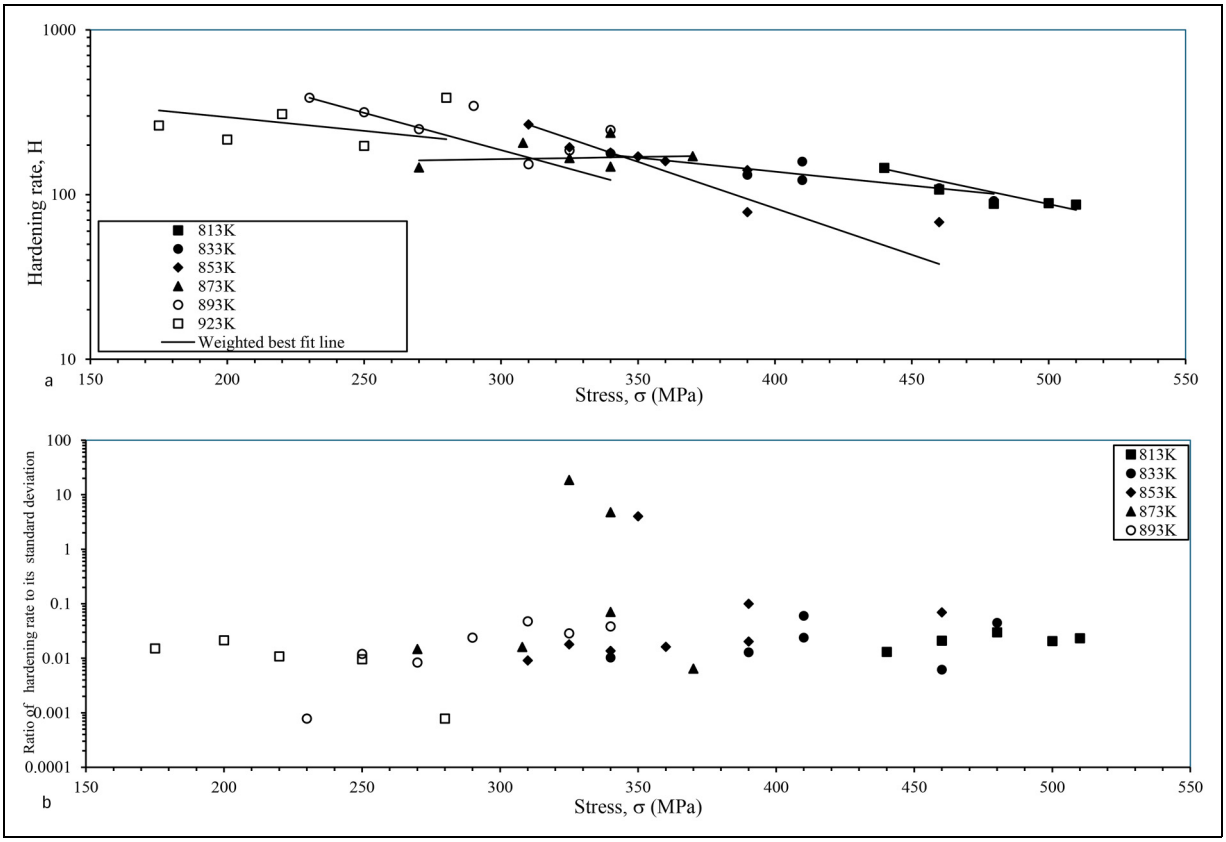

Figure 4. Variation of a. the estimates made for the hardening proportionality constant $\hat{H}$ with each test condition together with the weighted best fit iso-thermal lines, and b. the variation of the ratio of these estimates to their standard deviation with test conditions.

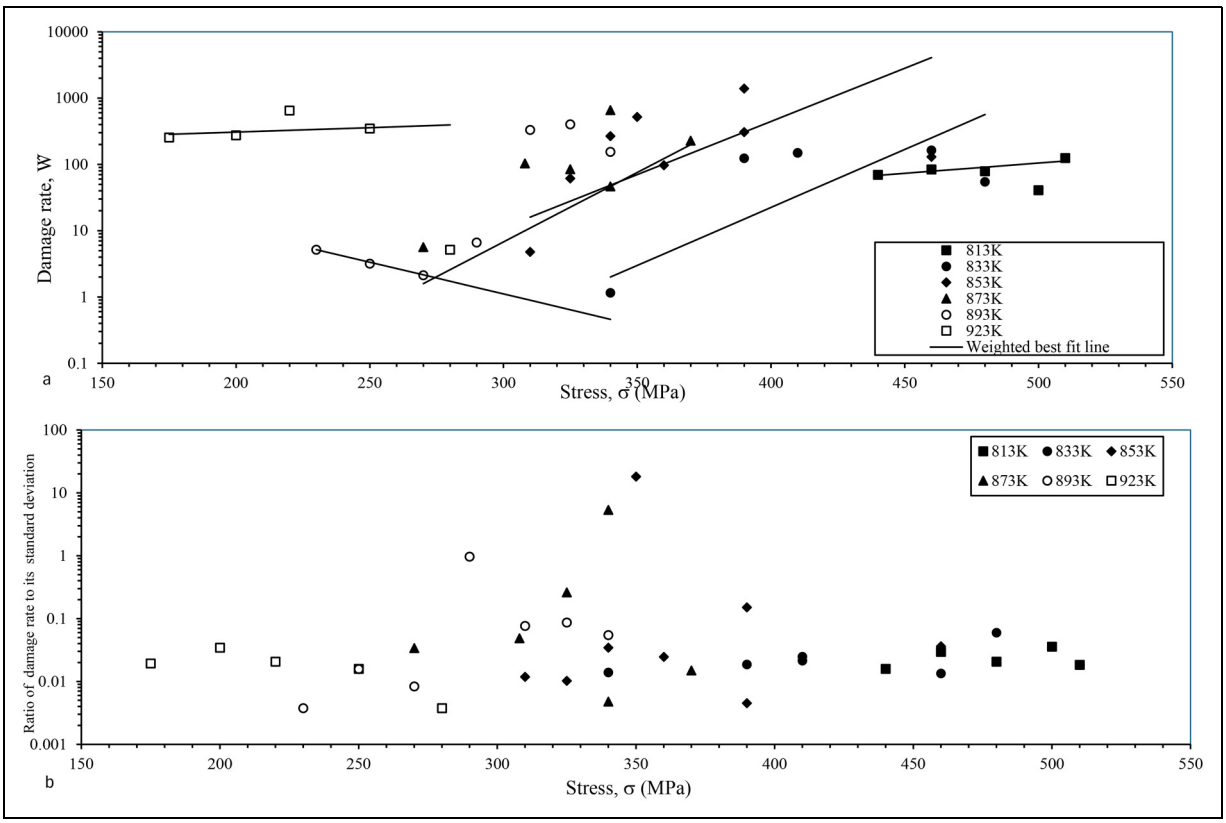

Figure 6. Variation of a. the estimates made for the damage proportionality constant $\hat{W}$ with each test condition together with the weighted best fit iso-thermal lines, and b. the variation of the ratio of these estimates to their standard deviation with test conditions.

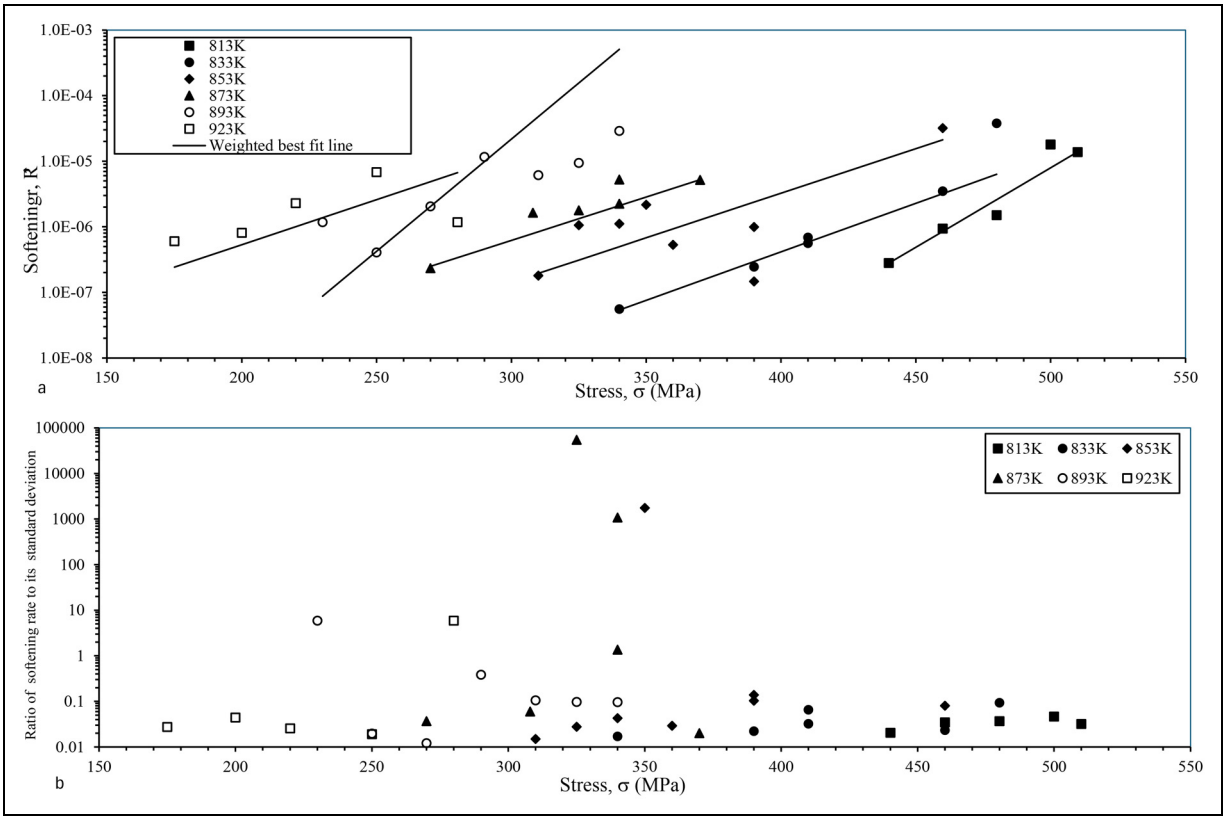

Figure 5. Variation of a. the estimates made for the softening proportionality constant $\hat{R}$ with each test condition together with the weighted best fit iso-thermal lines, and b. the variation of the ratio of these estimates to their standard deviation with test conditions.

complex interplay between stress, temperature, and microstructural evolution in these materials.

Several damage mechanisms have been identified for 9–12Cr steels. Parker[23] identified the nucleation of voids at precipitates and inclusions followed by growth and coalescence as a major damage mechanism – with void nucleation being influenced by the size and distribution of these precipitates and stress conditions. Pešička et. al.[21] found that 12% Cr steels exposed to service conditions displayed sub grain growth and precipitate coarsening – specifically the coarsening of precipitates like $M_{23}C_6$ and Laves phases. Void formation was particularly prevalent at high temperatures and moderate to high stresses, whilst coarsening and grain boundary sliding was confined to high temperatures with stress having only an indirect influence.

Figure 6(a) shows the estimates made for the proportionality constant determining the damage rate at each test condition, together with the weighted best fit iso-thermal lines. Figure 5(b) plots the ratio of each damage constant to its standard deviation are plotted. Unlike the hardening and softening rates, the damage rate does not appear to have any clear relationship with either stress or temperature. Although the figure plots the best fit lines, a possible interpretation of Figure 6(a) is that the damage constant is broadly independent of both stress and temperature, but that there are two broadly distinct levels. The first level corresponds to low damage constants of between 1 and 10 occurring mainly at the lowest recorded stresses and at the highest temperatures. This is consistent with the work carried out by Pešička et. al.[21] who found void formation required at least moderate stresses. The higher damage constants observed at the largest temperature of 923 K is also consistent with the work by Parker[23] who found nucleation of voids and coarsening was bigger at higher temperatures. Pešička et. al.[22] also found that coarsening was more prevalent at higher stresses – hence the relatively large values for the damage rate at the highest stresses in Figure 6(a).

Figure 7 plots the amount of damage accumulated by the time of failure against the proportionality constant for the rate of damage accumulation, and thus against the rate of damage accumulation for a given rate of strain. There is a clear relationship between these two variables: when damage accumulates rapidly, the result is a higher damage at failure. Low amounts of damage at failure accumulate at a low rate in other words.

Monkman Grant relation

When applying Equation (1a) to all the experimental data outlined in the data section, $\rho = 0.773$ and $M = 0.8048$. There is however a lot of variation around this relation, with it explaining only around 93% of the variation in failure times. There appears to be some points that appear to be well above the fitted line and some that are well below the line which may be an indication that the Monkman-Grant constant M is not truly constant.

The following subsections demonstrate that the data in Figure 8 fit into three distinctly different groupings depending on the value for M_2 and thus depending also on the tolerance to damage and the rate of damage accumulation. The statistical rational for such a grouping is provided in the failure time sub section below. Figure 9 plots the values for M_2 as calculated using Equations (10, 12), against stress

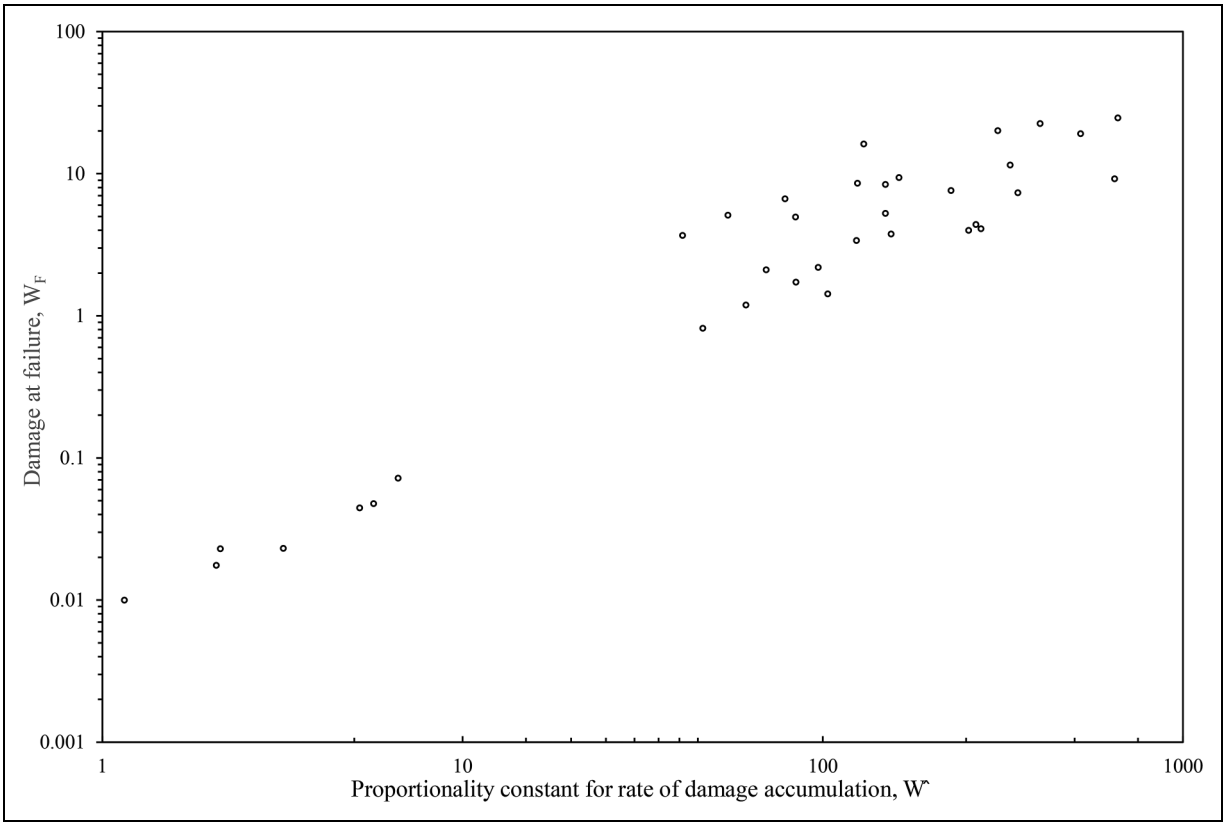

Figure 7. Relationship between damage at failure and rates of damage accumulation.

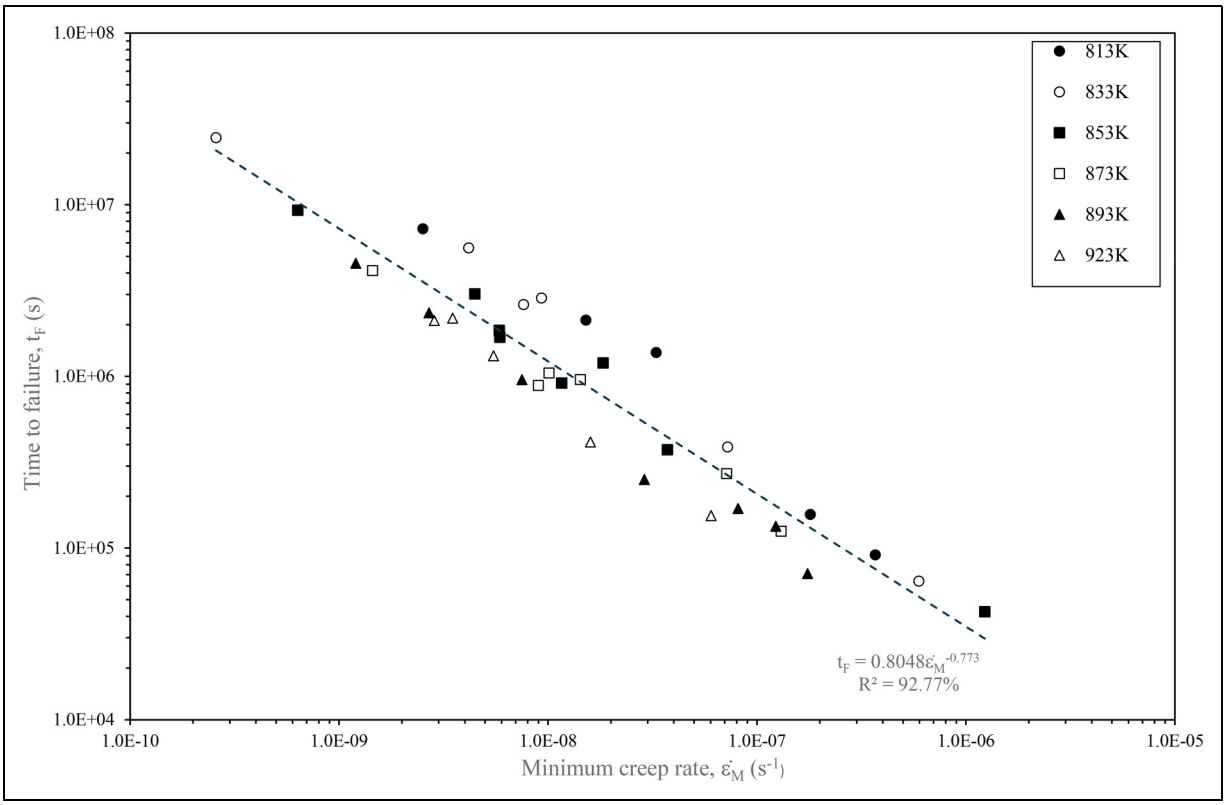

Figure 8. Variation in times to failure with measured minimum creep rates, together with the least squares regression line.

with the different symbols differentiating further with respect to temperature. Group 1a corresponds to test conditions producing M_2 values below 0.73%, whilst Group 1c corresponds to test conditions producing M_2 values above 1.7%. Group 1b corresponds to test conditions producing M_2 values in between these two limiting values.

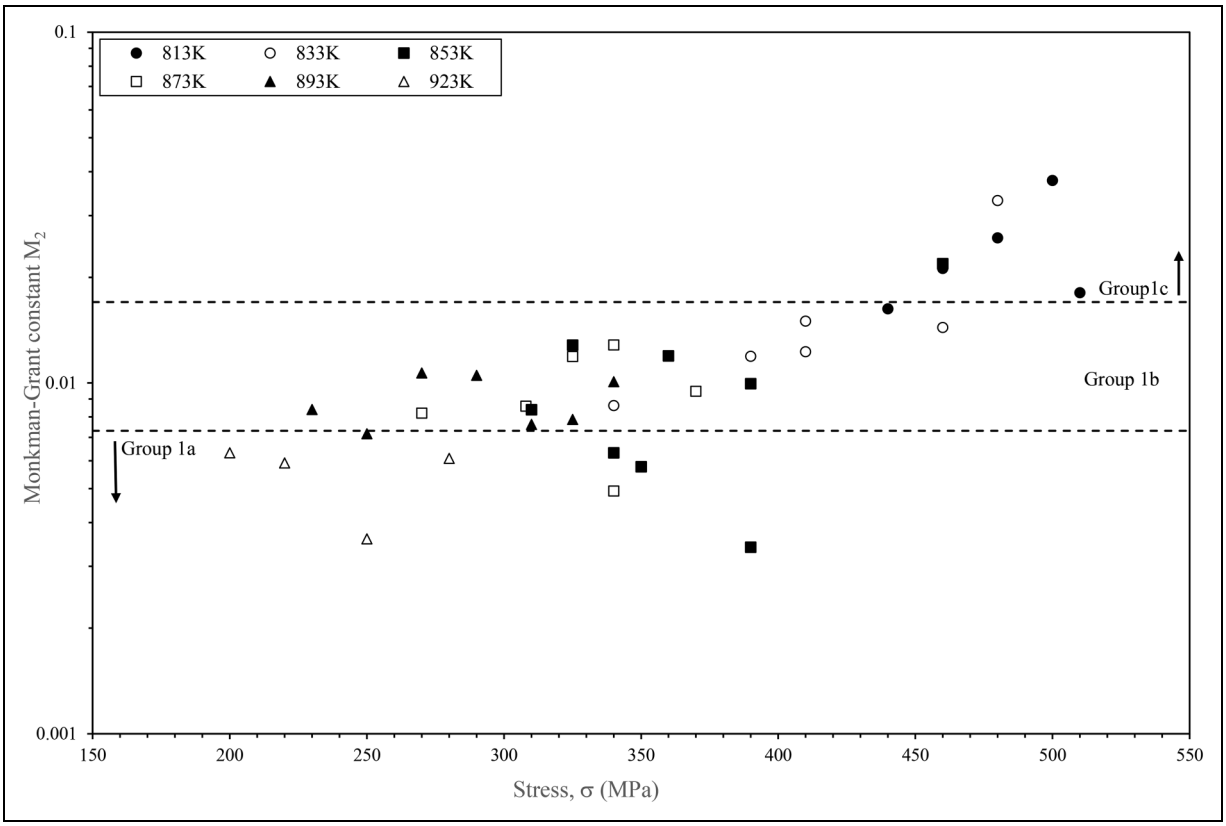

Figure 9. Variations in M_2, as calculated using Equation (10), with stress and temperature.

Group 1c: Highest values for M_2

Six data points make up this group and they correspond to the lowest three temperatures used in this test programme. They also correspond to the largest stress used at 833 K and 853 K and all but the lowest stress used at 813 K. Thus, relatively high M_2 values are generated by high stresses at low temperatures. Figure 10 shows the creep curves corresponding to four of the six data points making up group 1c. The two creep curves obtained at 813 K (Figure 10(a), (b)) had almost identical levels of tertiary strain, but the specimen tested at 480 MPa, could tolerate nearly twice the amount of damage before failing. Yet both specimens had high M_2 values, which can be explained by the fact the specimen tested at 480 MPa accumulated damage at almost twice the rate of the specimen test at 500 MPa. The specimen tested at 853 K (Figure 10(d)) could tolerate a large amount of damage before failing yet had an M_2 value almost the same as the specimen tested at 480 MPa and 813 K (Figure 10(b)). This is because the damage in the specimen tested at 853 K had over twice the rate of damage accumulation than that experienced by the specimen tested at 480 MPa and 813 K.

Group 1a: Lowest M_2 values

The low M_2 values associated with this group are generated either by the two highest temperatures irrespective of stress, or at stresses below 390 MPa at a temperature of 853 K. This is because at 853 K M_2 appears to be stress dependent but at the higher temperature of 923 K it is not. Figure 11 shows the creep curve corresponding to one data points making up group 1a. Now if we compare the Figure 11 with Figure 10(a), it becomes clear that these two test conditions result in similar tolerances to damage – (4.4 and 3.7). The specimen in Figure 10(a) has a much higher M_2 value because it has a much lower rate of damage accumulation (41 compared to 266).

The data in Figures 12 provides a further insight into the fundamental characteristics of the data points in this and the low M_2 value group. Figure 12(b) plots values for M_2 against W_F and the data in groups 1a and 1c have broadly similar W_F values – in group 1a W_F is scattered around a mean value of 8, whilst in group 1c W_F is scattered around a mean value of 20. Yet the data in group 1c have much higher M_2 values compared to those in group 1a. Figure 12(a), which plots values for M_2 against $\hat{W}$, explains why. It is the result of the rate of damage accumulation being much lower in group 1c compared to group 1a – an average of 85 compared to 485. And as Equation (10) reveals, lower values for $\hat{W}$ results in larger M_2 (and failure time) values.

Thus, a high value for M_2 is caused by a relatively high damage at failure and a relatively low rate of damage accumulation. Consequently, with a high tolerance to damage and a slow rate of damage accumulation the time to failure will be large, i.e., M_2 is high so that at a given secondary creep rate failure times will be high in this group. Such characteristics are generated by high stresses at low temperatures. A low value for M_2 is caused by a relatively high damage at failure with a relatively high rate of damage accumulation. Consequently, even though there is a high tolerance to damage, the higher rate of damage accumulation reduces the time taken to fail, i.e., M_2 is low so that at a given secondary creep rate, failure times will be lower in this group. Such

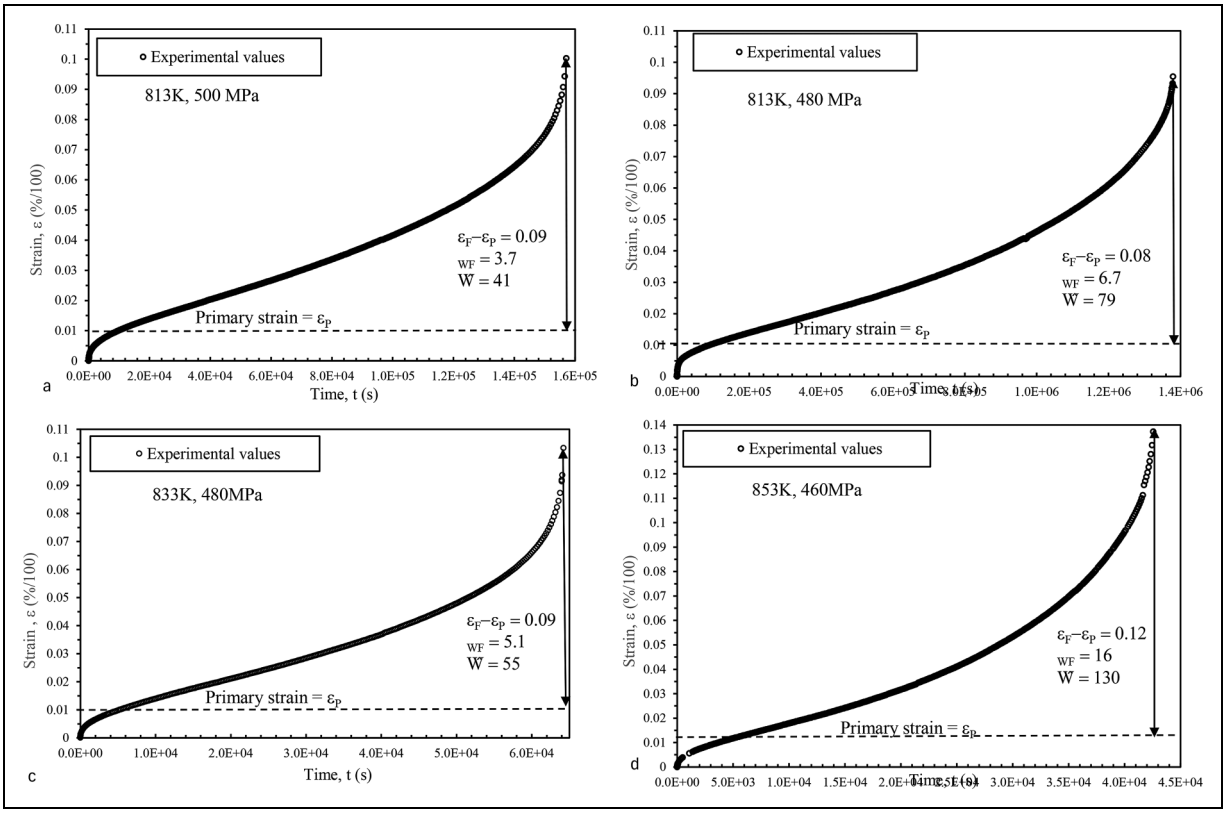

Figure 10. Creep curves with M_2 values above 1.7%. a. at 813 K and 500 MPa, b. 813 K and 480 MPa, c. 833 K and 480 MPa and d. 853 K and 460 MPa.

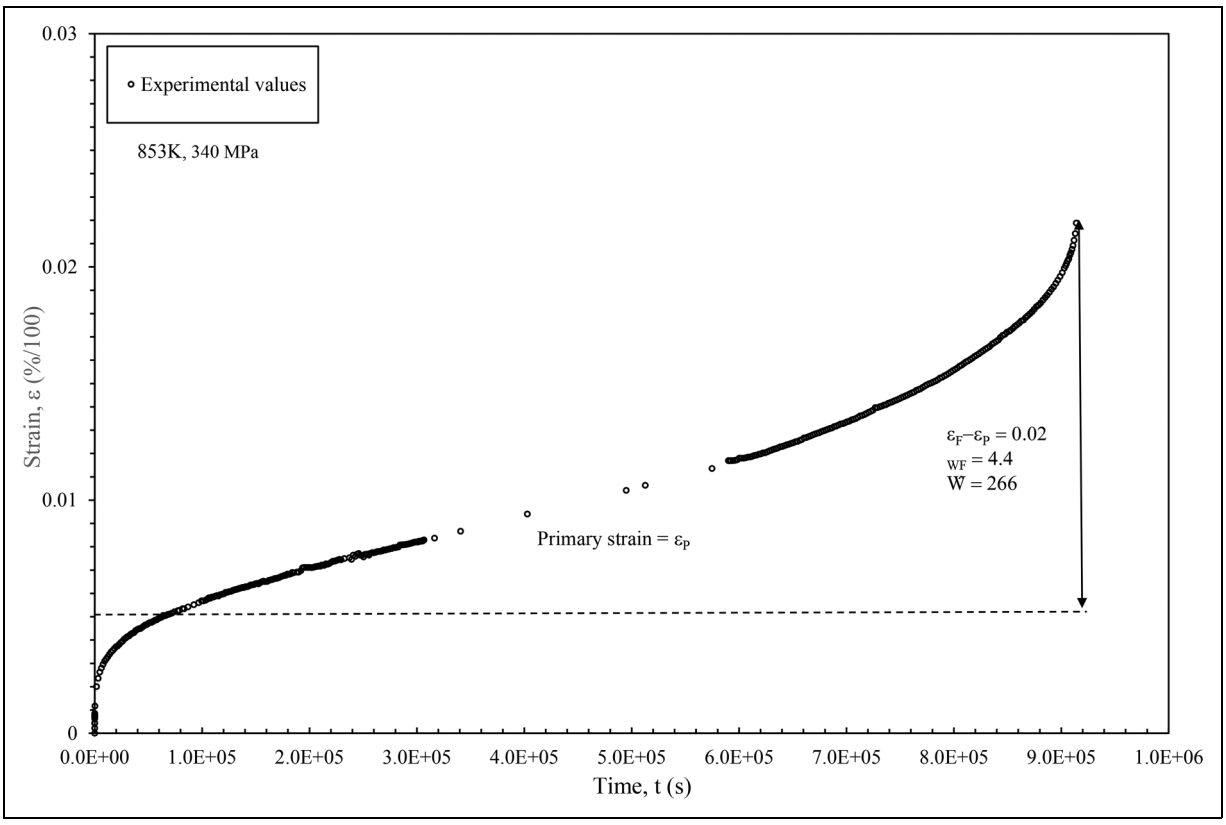

Figure 11. A creep curve with an M_2 value below 0.95% obtained at 833 K and 390 MPa, and b. 853 K and 340 MPa.

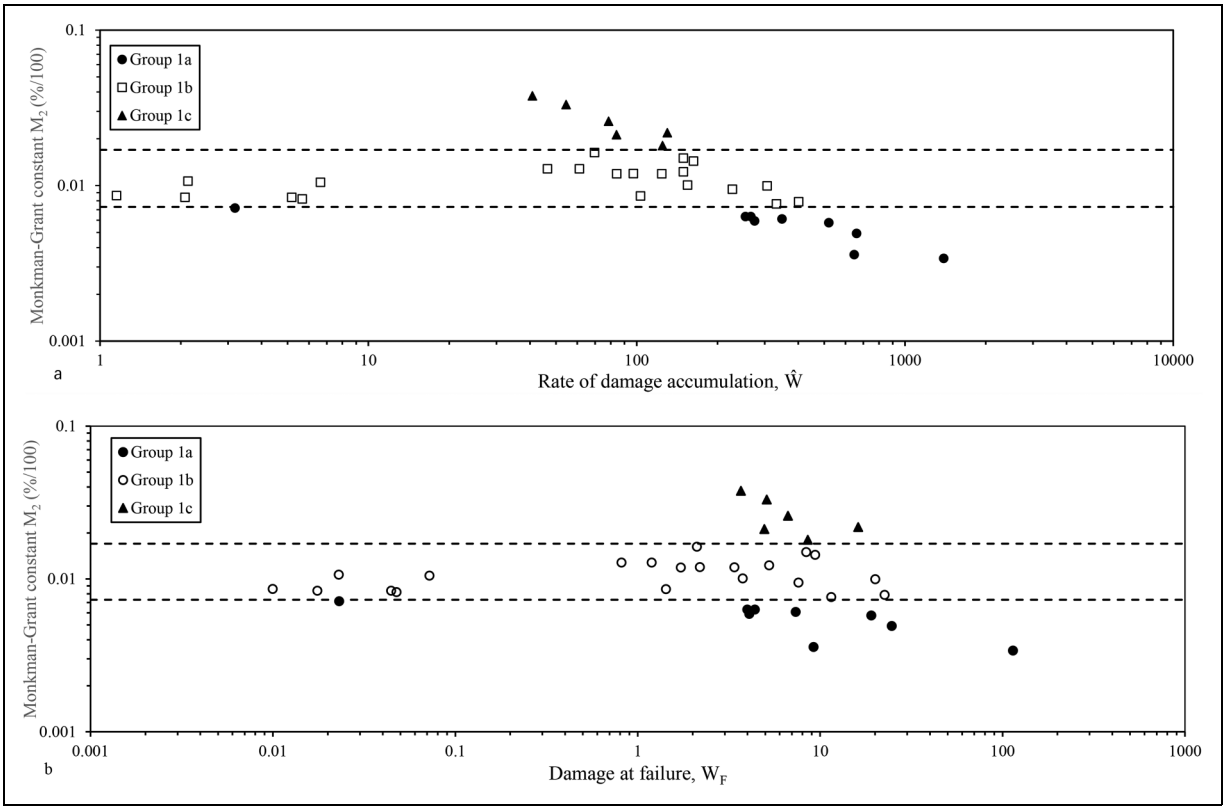

Figure 12. Variation in the Monkman-Grant constant M_2 values with a. the proportionality constant for rates of damage accumulation $\hat{W}$ and b. amounts of damage at failure W_F.

characteristics are generated by low stresses at a high temperature or moderately used stresses at a moderately used temperature.

Group 1b: Intermediate M_2 values

The data points making up this group correspond to all but the highest temperature used −923 K – and stresses below 410 MPa. The specimen tested at the lower of these temperatures (Figure 13(a)) tolerated twice the amount of damage, but this damage occurred at only 15% of the rate experienced by the specimen tested at the higher temperature (Figure 13(b)), resulting in these two specimens having intermediate M_2 values. Then if we compare the Figure 13(b) with Figure 10(b), it becomes clear that these two test conditions result in almost identical rates of damage accumulation – (79 and 84). The specimen in Figure 10(b) has a higher M_2 value because it has higher tolerance to damage (6.7 compared to 1.7).

Figures 12 reveals there are two distinctly different creep characteristics generating the intermediate values for M_2. The first group has values for W_F that are like those in groups 1a and 1c, but these intermediate values for M_2 are then generated by $\hat{W}$ values in between those for groups 1a,c. The second grouping is more interesting, as the intermediate values for M_2 are generated by much lower values for W_F compensated for by much lower rates of damage accumulation so still leading to a intermediate value for M_2. Figure 14 illustrates what low values for W_F and $\hat{W}$ look like in terms of actual rates of creep. The creep rates in this figure are calculated using Equation (11) and show the rates of creep for four of the seven data points that have very low W_F and $\hat{W}$ values. These creep curves were generated by the lowest stress used at temperatures 823 K, 853 K and 873 K, but the highest stresses used at 893 K. (Note one of these seven data points could belong to either group 1a and 1b and so its assignment to group 1a could easily be changed without altering the results in a significant way). What is interesting about this grouping is that the short periods of primary creep followed by long periods of constant creep rates with little or no accelerating creep rates is typical of longer-term tests carried out at stresses much lower than those used in this paper. As such the Monkman-Grant relation from this intermediate M_2 grouping might be relevant for longer term life assessment based on early data on minimum rates at very low stress conditions.

Figure 15 plots damage at failure against stress with a demarcation with respect to temperature also shown for all the data points making up group 1b. The very low amounts of damage at failure occur at the lowest stresses recorded at temperatures below 923 K. Further this move to very low amounts of damage, occurs at a stress of around 310 MPa. In the literature there is also some fractographic and microstructural evidence to support this pattern. Xu et. al.[24] found that at stresses below ~340 MPa, dislocation-controlled creep dominates, precipitate coarsening is limited, and void nucleation is scarce—thus rupture occurs with minimal mesoscale damage and retains ductility. At higher stresses, these authors found that diffusional and grain-boundary driven damage accelerates. More specifically, Laves-phase coarsens, MX dissolves, void nucleation becomes widespread along boundaries, and damage localizes—leading to failure with significant damage signatures.

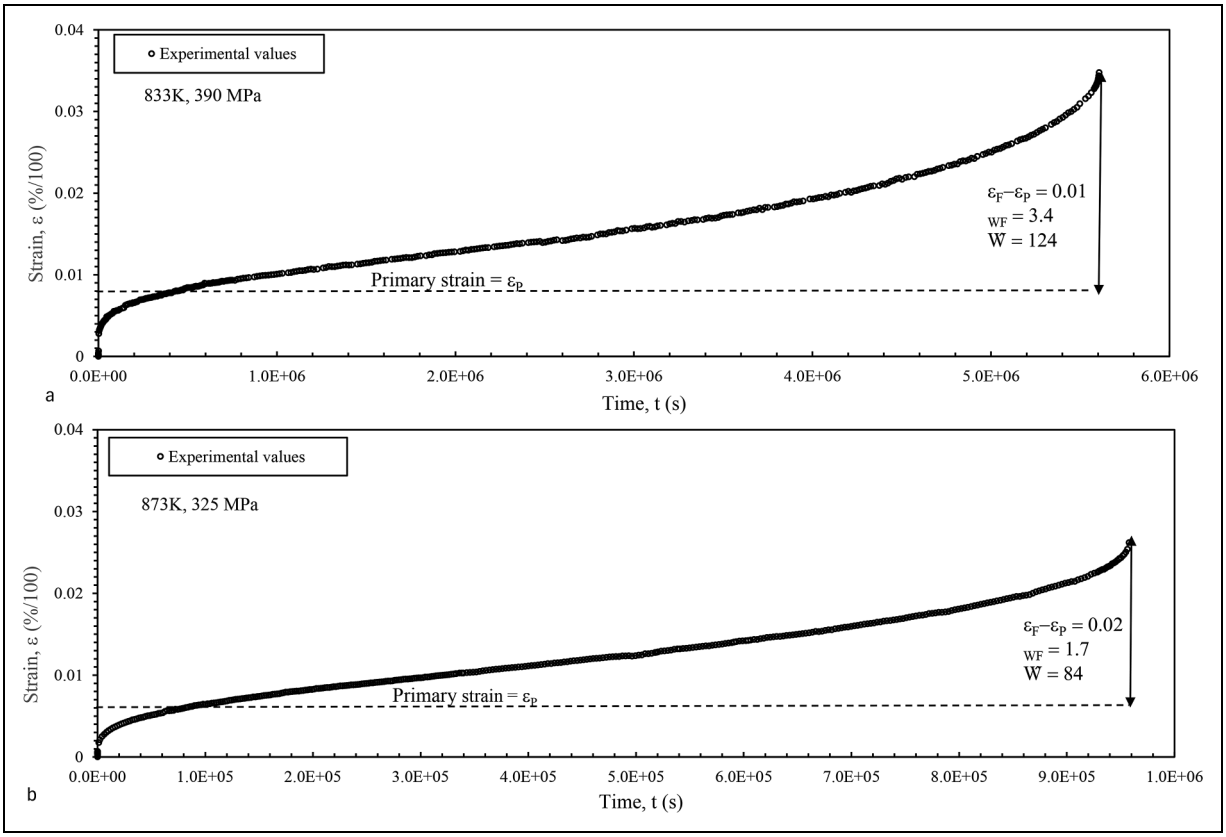

Figure 13. Some creep curves with M_2 values below 1.7% but above 0.73%. a. at 833 K and 390 MPa, and b. 873 K and 325 MPa.

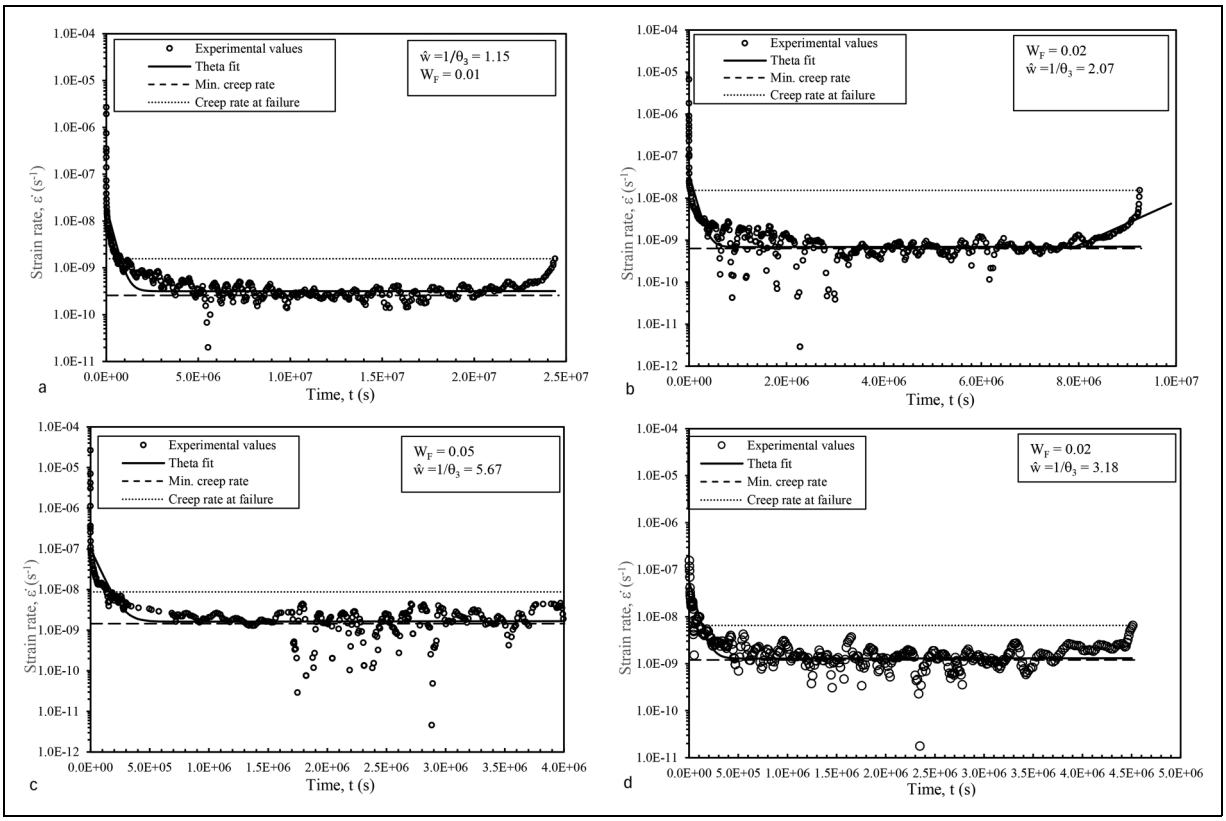

Figure 14. Variations in rates of creep with time for specimens tested at a. 833 K with 340 MPa, b. 853 K with 310 MPa, c. 873 K with 270 MPa and d.893 K with 250 MPa.

These authors also found that at stresses around 100–190 MPa, void densities are low and isolated with typical sizes ~4–6 μm in diameter. Fractography revealed dimpled, ductile trans granular fracture with sparse cavities nucleated at coarse precipitates (e.g., Laves clusters). These void densities correspond to cavity area fractions well below ~0.3%,

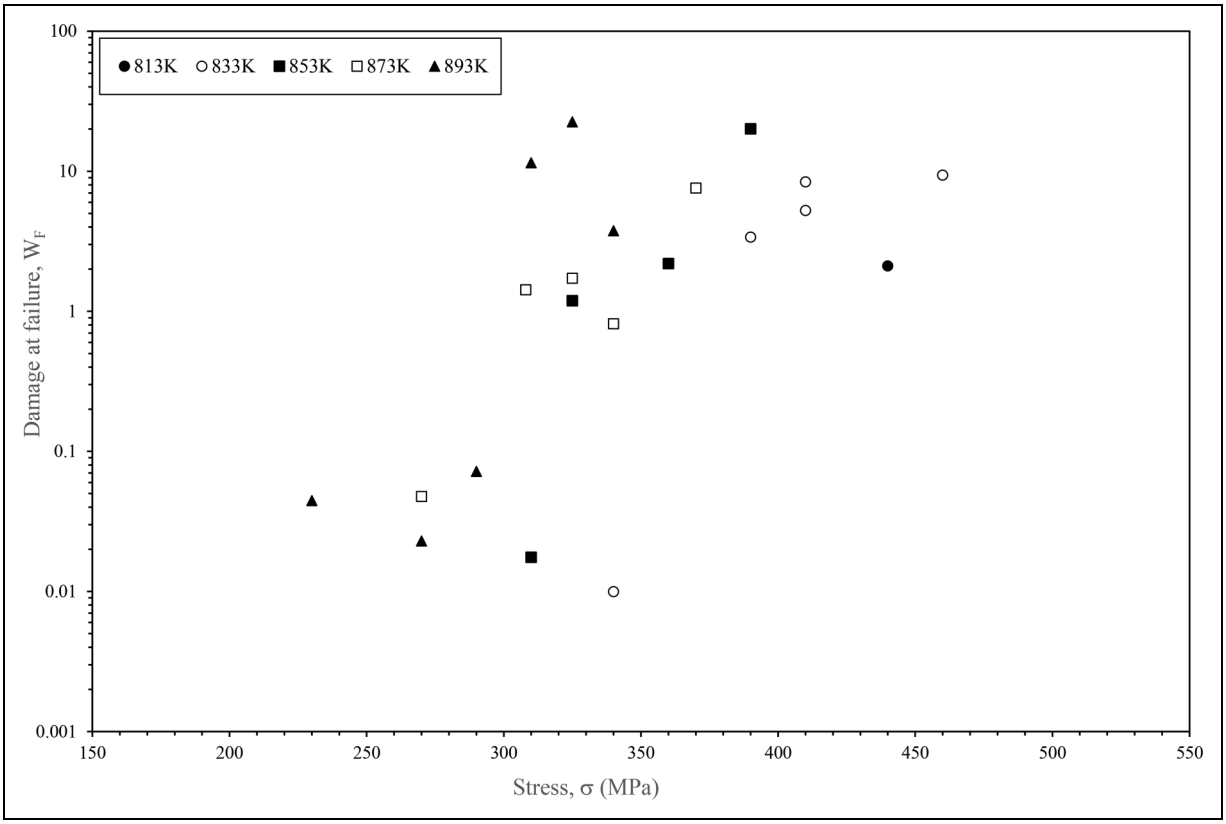

Figure 15. Variation of damage at failure with stress and temperature.

indicating minimal damage at failure. Yan et. al.[25] found that at stresses of ≥ 300–400 MPa, void density and size escalate sharply. SEM fractography showed large clusters of cavities and cavity bands aligned along grain boundaries, typical of creeping along prior-austenite grain boundary zones. Fracture surfaces shift to mixed or intergranular modes, with visible cavity coalescence and secondary cracking.

Failure times

The statistical justification for the subgroupings shown above, is that the mean values for M_2 in each group are statistically significantly different from each other. When using mean values, such statistical significance can be tested using the following t-value

$$\text{t} - \text{value} = \frac{(\bar{M}_{2,1} - \bar{M}_{2,2}) - (\mu_1 - \mu_2)}{\sqrt{\frac{s_1^2}{n_1} + \frac{s_2^2}{n_2}}} \qquad (13a)$$

where μ_1 is the population (true) mean value for M_2 for damage conditions that place results within one of the three groups seen in Figure 9 and μ_2 is the population (true) mean value for M_2 for damage conditions that place results within another of the three groups seen in Figure 9. This test statistic allows for unequal variances between the groupings. $\bar{M}_{2,1}$ and $\bar{M}_{2,2}$ are the corresponding estimated means from samples of size n_1 and n_2. s_1^2 and s_{22} are the sample variances that can be estimated using the sample variance formula. Under the null hypothesis that the true mean values for M_2 are the same between two groups (Ho: $\mu_1 - \mu_2 = 0$), this t-value follows (approximately) a student t distribution with degrees of freedom (d.f.) estimated as

$$\text{d.f.} = \frac{\left(\frac{s_1^2}{n_1} + \frac{s_2^2}{n_2}\right)^2}{\frac{1}{n_1 - 1}\left(\frac{s_1^2}{n_1}\right)^2 + \frac{1}{n_2 - 1}\left(\frac{s_2^2}{n_2}\right)^2} \qquad (13b)$$

These t-values for mean comparisons are shown in the one but last column of Table 4. Thus, the t-value of −4.90 tests the null hypothesis that the difference between the true mean values for M_2 in group 1a and group 1c are the

Table 4. Mean values for M_2 in each grouping, together with tests for the statistical significance of differences between these means.

Group	Monkman-Grant constant M_2				
	Mean	Standard Deviation	d.f.	t-value	p-value
Group 1a	0.0055	0.00128	27	−7.72[a]	3.39E-08
Group 1b	0.0108	0.00249	5	−4.90[b]	0.0045
Group 1c	0.0263	0.00763	5	−6.62[c]	0.0012

d.f. is the degrees of freedom as calculated using Equation (13). p-value is the probability that there is no difference between the population mean values in the groupings listed below:

[a]This is the student t statistic for testing for a statistically significant difference between the population mean value for M_2 in group 1a and group 1b.

[b]This is the student t statistic for testing for a statistically significant difference between the population mean value for M_2 in group 1a and group 1c.

[c]This is the student t statistic for testing for a statistically significant difference between the population mean value for M_2 in group 1b and group 1c.

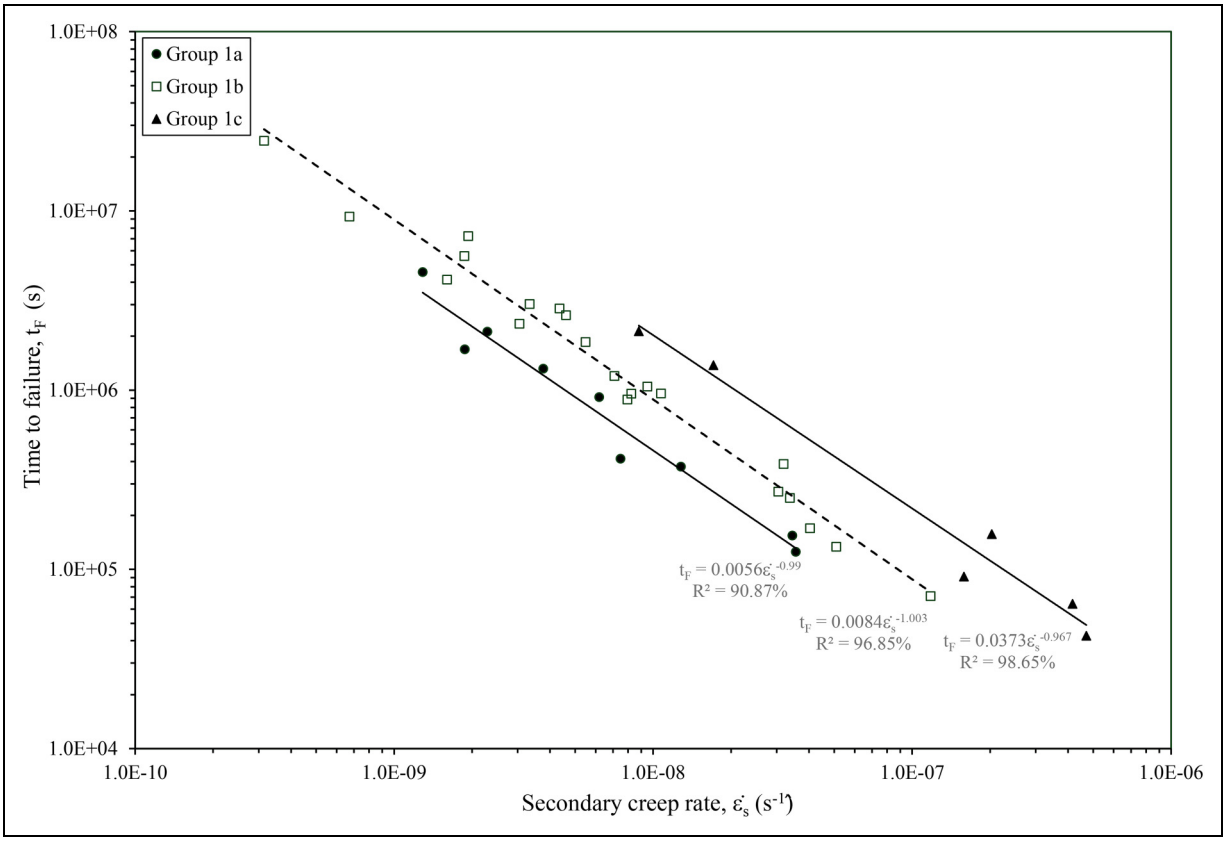

Figure 16. Variations in time to failure with the secondary creep rate, together with the estimated Monkman-Grant relation for each group of data.

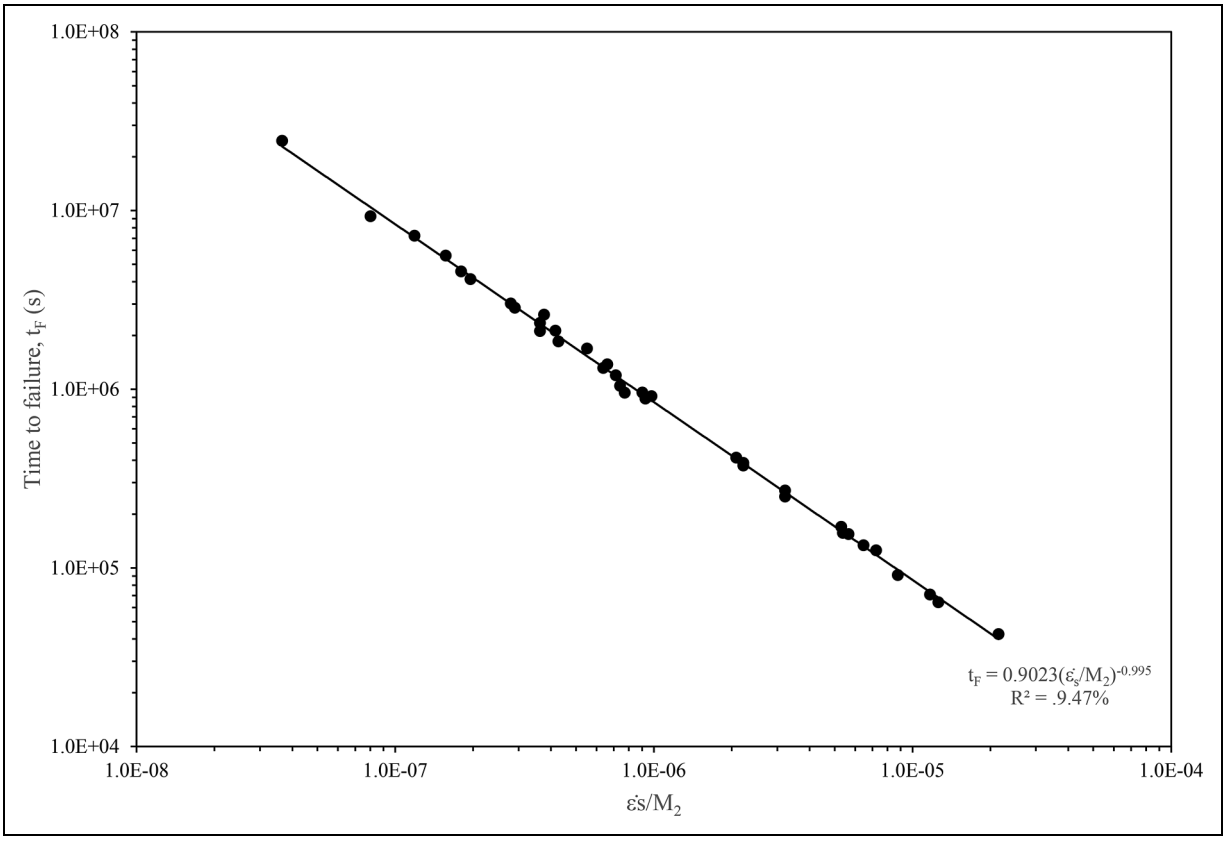

Figure 17. The modified 4-θ Monkman-Grant relation.

same. Based on the t-value, the probability that this null hypothesis is true is 0.45%. So, at the 1% significance level, the mean value for M_2 in these two groups are different, i.e., the negative value for the sample mean difference of (0.0055–0.0263) has not occurred by chance. Table 4 reveals that the three mean values are all statistically significantly different from each other at the 1% significance, so that the best fit lines in Figure 16 differ from each other in a statistically significant way.

Figure 16 shows the estimates made for the parameters of the Monkman-Grant relation of Equation (10) within each of the groupings identified above. The Monkman-Grant constant M_2 increases from 0.56% in group 1a to 0.84% in group 1b and to 3.73% in group 1c. These significant differences take the form of a parallel shift as damage characteristics change. That is, $\rho = 1$ in all three groupings. Even in group 1c where ρ is estimated at 0.97, this is not significantly different from 1 – the p-value for the null hypothesis that the true value for ρ is 1 is 64.8%. There is therefore a very high probability that the true value for ρ is 1 (it would come out as 1 if there were many more data points available). The p-values for testing $\rho = 1$ in the other two groups are 55.5% for group 1a and 46.6% for group 1b. Thus, once account is taken for different amounts and rates of damage accumulation, the true value for ρ is 1, irrespective of these differences in damage. $\rho = 1$ is as predicted by the 4-θ methodology.

To further confirm the validity of the 4-θ Monkman-Grant relation, the data points of Figure 16 are replotted in Figure 17 according to Equation (10). The gradient of -0.995 of the regression line in Figure 17 corresponds to the exponent on $\dot{\varepsilon}_S$ in Equation (10) and so is as predicted by the 4-θ methodology. The proportional coefficient of 0.902 is close to the value of 1 that is predicted by the 4-θ methodology. Indeed, the p-value for testing that the population value for this proportional coefficient equals 1 comes out at 28% and so this hypothesis cannot be rejected – even as the 10% significance level. Unlike in Figures 8 and 16, all the data points are closely packed around one regression line, contrary to their larger deviations in Figure 8 around a single regression line and around multiple lines in Figure 16. The scatter in data points is also dramatically reduced in Figure 17 as compared with Figures 8 and 16.

Conclusions

The Monkman-Grant relation offers the possibility of reducing the cost and length of the development cycle for new materials operating at high temperatures by using minimum creep rates that can be obtained relatively quickly even at low stresses. This paper used the 4-θ methodology to i. identify and explain the form of this relation in terms of creep mechanisms such as hardening, recover and damage and ii. to discover whether this form was compatible with long term creep life assessment. The 4-θ methodology suggests that the traditionally measured minimum creep rate should be replaced by the theoretical minimum creep rate measured as $\theta_3\theta_4$, It also predicts that the exponent on this secondary creep rate will equal -1. This methodology also predicted that the Monkman-Grant proportionality constant (M_2) was positively related to the amount of strain during tertiary creep, positively related to the total amount of damage accumulated during this stage but negatively related to the rate at which damage accumulates. The methodology also suggested that the role played by primary creep in identifying the form of the Monkman-Grant relation was restricted to the determination of the theoretical secondary creep rate.

These predictions were confirmed by the data obtained on 12Cr-Mo-V-Nb steel. Without considering any of these causal variables, the exponent on the minimum creep rate was considerably different from the 4-θ prediction that it should equal -1 (-0.77). However, it was also found that the values for the Monkman-Grant proportionality constant (M_2) fell into three well defined groupings depending on the amount of accumulated damage and the rate at which it occurred. Two of the groupings had similar amounts of damage at failure, but different rates of damage accumulation that split the data into low and high M_2 values. It then turned out that within each such grouping, the exponent on the secondary creep rate equalled -1. The other grouping had rates of damage accumulation in between these two other groupings. However, this intermediate grouping also contained some results where both the amount of damage at failure and the rate at which it accumulated were very low (leading to an intermediate M_2 value). What is interesting about this grouping is that this damage characteristic is typical of longer-term tests carried out at stresses much lower than those used in this paper and much closer to typical operating stresses for this material. As such the Monkman-Grant relation from this intermediate M_2 grouping might be relevant for longer term life assessment based on early data on minimum creep rates at very low stress conditions. An interesting area for future research therefore is to study this possibility for reducing the development cycle for new materials in more detail.

Author contribution(s)

Mark Evans: Conceptualization; Formal analysis; Investigation; Methodology; Project administration; Writing – original draft; Writing – review & editing.

Funding

The author received no financial support for the research, authorship, and/or publication of this article.

Declaration of conflicting interests

The author declared no potential conflicts of interest with respect to the research, authorship, and/or publication of this article.

References

1. Yang M, Wang Q, Song XL, et al. On the prediction of long-term creep strength of creep resistant steels. *Int J Mater Res* 2016; 107: 133–138.
2. Wilshire B and Battenbough AJ. Creep and creep fracture of polycrystalline copper. *Mater Sci Eng, A* 2007; 443: 156–166.
3. Wilshire B and Scharning PJ. Prediction of long-term creep data for forged 1Cr-1Mo-0.25V steel. *Mater Sci Technol* 2008; 24: 1–9.
4. Wilshire B and Whittaker M. Long term creep life prediction for grade 22 (2.25Cr-1Mo) steels. *Mater Sci Technol* 2001; 27: 642–647.

5. Wilshire B and Scharning PJ. A new methodology for analysis of creep and creep fracture data for 9–12% chromium steels. *Int Mater Rev* 2008; 53: 91–104.
6. Whittaker MT, Evans M and Wilshire B. Long-term creep data prediction for type 316H stainless steel. *Mater Sci Eng A* 2012; 552: 145–150.
7. Monkman FC and Grant NJ. An empirical relationship between fracture life and minimum creep rate in creep rupture tests. *Proc Am Soc Test Mater* 1956; 56: 593–605.
8. Cocks ACF and Ashby MF. On creep fracture by void growth. *Prog Mater Sci* 1982; 27: 189–244.
9. Abe F. Creep behaviour, deformation mechanisms, and creep life of mod.9Cr-1Mo steel. *Metall Mater Trans: A* 2015; 46: 5610–5625.
10. Choudhary BK. Tertiary creep behaviour of 9Cr-1Mo steel. *Mater Sci Eng A* 2013; 585: 1–9.
11. Dobes F and Milicka K. The relation between minimum creep rate and time to fracture. *Metal Sci* 1976; 10: 382–384.
12. Sklenicka V, Kucharova K, Kral P, et al. Applicability of empirical formulas and fractography for assessment of creep life and creep fracture modes of tempered martensitic 9%Cr steel. *Kovove Mater* 2017; 55: 69–80.
13. Maruyama K, Sekido N and Yoshimi K. Changes in Monkman-Grant relation among four creep regions of modified 9Cr-1Mo steel. *Mater Sci Eng A* 2019; 749: 223–234.
14. Evans RW and Wilshire B. *Creep of metals and alloys*. London: Institute of Metals, Appendix, 1985.
15. Evans RW. A constitutive model for the high-temperature creep of particle-hardened alloys based on the Θ projection method. *Royal Soc Proc: Math Phys Eng Sci* 1996; 2000: 835–868.
16. Kafexhiu F, Vodopivec F and Podgornik B. Analysis of primary creep in simulated heat affected zone (HAZ) of two 9–12% cr steel grades. *Metalurgija* 2017; 56: 353–356.
17. Harrison W. *Creep modelling of Ti6246 and Waspaloy using ABAQUS*. PhD Thesis, University of Wales Swansea, UK, 2007.
18. Harrison W, Whittaker M and Gray V. Advanced methods for creep in engineering design. In: Tanski T, Sroka M and Zielinski A (eds) *Creep*. IntechOpen, 2018. Available at: https://doi.org/10.5772/intechopen.72319.
19. Evans RW. Statistical scatter and variability of creep property estimates in θ projection method. *Mater Sci Technol* 1989; 5: 699–707.
20. Han H, Shen J and Xie J. Effects of precipitates evolution on low stress creep properties in P92 heat-resistant steel. *Sci Rep* 2018; 8: 15411.
21. Pešička J, Ghajani A, Somsen C, et al. How dislocation substructures evolve during long-term creep of a 12% cr tempered martensitic ferritic steel. *Scr Mater* 2010; 62: 353–356.
22. Dudova N. 9–12% Cr heat-resistant martensitic steels with increased boron and decreased nitrogen contents. *Metals (Basel)* 2022; 12: 1119.
23. Parker J. Component relevant creep damage in tempered martensitic 9 to 12%Cr steels. In: Advances in materials technology for fossil power plants: proceedings from the eighth international conference, Algarve- Portugal, 2016.
24. Xu Q, Lu Z and Wang X. Damage modelling: the current state and the latest progress on the development of creep damage constitutive equations for high Cr steels. *Energy Mater* 2017; 12: 229–237.
25. Yan K, Cai Y, Wang D, et al. Prediction of residual life of in-service P91 steel joints based on fracture behaviour. *Materials (Basel)* 2024; 17: 2789.

Appendix I

Here a short confirmation that the derivative of M_2 with respect to $\hat{W}$ is negative. From Equation (10)

$$M_2 = \frac{1}{\hat{W}}\ln[1 + W_F] = \frac{1}{\hat{W}}\ln[1 + \hat{W}\mathrm{x}\,] \qquad (A1)$$

where $\mathrm{x} = (\varepsilon_F - \varepsilon_p)$. Using the quotient rule for differentiation

$$\frac{\mathrm{dM}_2}{d\hat{\mathrm{W}}} = \frac{\dfrac{\hat{\mathrm{W}}x}{1 + \hat{\mathrm{W}}x} - \ln[1 + \hat{\mathrm{W}}x]}{\hat{\mathrm{W}}^2} \qquad (A2)$$

Next, define $\mathrm{u} = \hat{\mathrm{W}}x$ and h(u) as

$$\mathrm{h}(u) = \hat{\mathrm{W}}^2\frac{\mathrm{dM}_2}{d\hat{\mathrm{W}}} = \frac{u}{1+\mathrm{u}} - \ln[1+\mathrm{u}] \qquad (A3)$$

It needs to be shown that $\mathrm{h}(\mathrm{u}) < 0$ for all $\mathrm{u} >= 1$, $\mathrm{u} \neq 0$ because $\ln(1+\mathrm{u})$ is only defined for $\ln(1+\mathrm{u}) > 0$. The derivative of h(u) with respect to u is

$$\frac{dh(u)}{\mathrm{du}} = \frac{-u}{(1+u)^2} \qquad (A4)$$

So, if $\mathrm{u} > 0$ then $\frac{dh(u)}{\mathrm{du}} < 0$ and so this derivative function is decreasing in u. If $\mathrm{u} < 0$ then $\frac{dh(u)}{\mathrm{du}} > 0$ and so this derivative function is increasing in u. Further, $h(0) = 0$, $h(u) < 0$ when $\mathrm{u} > 0$ and $h(u) < 0$ when $\mathrm{u} < 0$. Therefore

$$\mathrm{h}(u) = \frac{u}{1+\mathrm{u}} - \ln[1+\mathrm{u}] < 0 \quad \text{for} \quad \mathrm{u} > 0 \qquad (A5)$$

and thus

$$\frac{\mathrm{dM}_2}{d\hat{W}} = \frac{f(u)}{\hat{\mathrm{W}}^2} = \frac{f(\hat{\mathrm{W}}x)}{\hat{\mathrm{W}}^2} < 0 \qquad (A6)$$

Appendix 2

Table A. Nomenclature for all the symbols

Variable/constant	Description
t	Time
t_F	Time at failure
t_p	Time to reach the end of the primary creep phase
t_M	Time to reach $\dot{\epsilon}_M$
ϵ_F	Strain at failure
ϵ_p	Strain by time t_p
ϵ^	Rate of strain
t_i	ith measured time (of which there are n on a measured creep curve)
ϵ_i	ith measured strain
$\dot{\epsilon}_i$	ith measured strain rate
$\dot{\epsilon}_o$	Initial creep rate
$\ddot{\epsilon}$	Rate of change in ϵ^
σ	Stress, MPa
T	Temperature, K
$\dot{\epsilon}_M$	Minimum creep rate
$\dot{\epsilon}_S$	Secondary creep rate ($=\widehat{R}/\hat{H}$)
$\dot{\epsilon}_T$	Rate of tertiary creep
$\ddot{\epsilon}_T$	Rate of change in the tertiary creep rate
$\dot{\epsilon}_i$	ith measured creep rate
$\hat{R}$	Proportionality constant for the overall rate of softening
$\hat{H}$	Proportionality constant for the overall rate of hardening
$\hat{W}$	Proportionality constant for the overall rate of damage
R	Overall softening
H	Overall hardening
W	Overall damage accumulation
h_α	Individual hardening variable
r_α	Individual hardening variable
w_α	Individual hardening variable
$\hat{h}_\alpha$	Proportionality constant for an individual rate of hardening
$\hat{r}_\alpha$	Proportionality constant for an individual rate of softening
$\hat{w}_\alpha$	Proportionality constant for an individual rate of damage
$\dot{H}$	Rate of overall hardening
$\dot{R}$	Rate of overall softening
$\dot{W}$	Rate of overall damage
$\dot{h}_\alpha$	Rate of individual hardening
$\dot{r}_\alpha$	Rate of individual softening
$\dot{w}_\alpha$	Rate of individual damage
W_F	Damage accumulated at failure
θ	Theta parameter
M	Monkman-Grant proportionality constant
ρ	Monkman-Grant exponent
M_1	Dobes and Milicka Monkman-Grant proportionality constant
ρ_1	Dobes and Milicka Monkman-Grant exponent
λ	Damage tolerance parameter
A,B, α, b	Maruyama et al.[13] creep curve parameters
ξ_α	Internal state variable
$\Phi()$, $f(\xi_\alpha)$	Functional forms
C	Constant of integration
M_2	Monkman Grant proportionality constant implied by the Theta methodology
$\tilde{\theta}$	Estimate of θ
$\bar{M}_{2,1}$	Sample mean value for M_2 in group 1
μ_1	Population mean value for M_2 in group 1
s_1^2	Sample variance in the M_2 values in group 1
d.f.	Degrees of freedom